TRANSPORT IN DILUTE ALLOYS

TRANSPORT IN DILUTE ALLOYS

By

JOHN A. MASON, B.SC.

A Thesis

Submitted to the School of Graduate Studies

in Partial Fulfilment of the Requirements

for the Degree

Master of Science

McMaster University

January 1974

MASTER OF SCIENCE (1974) McMASTER UNIVERSITY
(Physics) Hamilton, Ontario.

TITLE: Transport in Dilute Alloys

AUTHOR: John A. Mason, B.Sc. (Royal Military College)

SUPERVISOR: Professor J. P. Carbotte

NUMBER OF PAGES: (iv), 93

SCOPE AND CONTENTS:

In essence this work is a study of transport properties of dilute alkali alloy systems and the numerical methods used to study them. The first chapter deals with the theory of lattice dynamics and the methods, based on this theory, of calculating phonon frequency distributions. These distributions are subsequently used to determine properties of alkali alloy systems.

Chapter II examines the use of the Ashcroft pseudopotential. Different types of screening are considered and the effects of adding many body corrections are examined.

A study of alkali alloy systems is undertaken in the third part of the work. Impurity theory is considered and calculations are undertaken for several alkali dilute alloy systems. Finally the results of the impurity calculations are examined for deviations from Matthiesen's rule.

ACKNOWLEDGEMENTS

I wish first to thank my supervisor, Dr. J. P. Carbotte, for his guidance and encouragement throughout the work. Also the advice and assistance of Dr. P. Truant was very helpful.

Much of the theory could not have been done without the assistance of Dr. F. Kus, and his help is gratefully acknowledged. Mr. P. Dunmore's assistance with computing was also much appreciated.

Special thanks must go to Miss Erie Long for her accurate typing of the manuscript and for her amazing patience. The financial assistance of McMaster University in the form of a McMaster Graduate Fellowship is gratefully acknowledged.

TABLE OF CONTENTS

CHAPTER I

PHONON FREQUENCY DISTRIBUTIONS

1.1 General Theory

In this Chapter we discuss the problem of lattice dynamics and the sources of data about the phonons. The numerical methods used to construct weighted phonon frequency distributions are considered and the Chapter concludes with a detailed discussion of the computer programme used to calculate isotropic weighted phonon frequency distributions.

The calculations are empirically based in that information concerning the phonons is gained from inelastic neutron scattering. Dispersion curves are established in this way for high symmetry directions in the first Brillouin zone (FBZ). It is then possible to fit a set of force constants for several nearest neighbour shells using the Born-von Kármán model. This is done in such a way that the fitted force constants can be used to obtain the phonon modes, to a high degree of accuracy, for both the high symmetry and off symmetry directions throughout the FBZ.

Using the harmonic approximation the classical equation of motion for the ℓth ion is,

$$- M\ddot{u}_{\alpha}(\ell) = \sum_{\beta\ell'} \Phi_{\alpha\beta}(\ell,\ell')u_{\beta}(\ell') \quad , \tag{1.1}$$

where $u_{\alpha}(\ell)$ is the αth component of the excursion from equilibrium of the ℓth ion and $\Phi_{\alpha\beta}(\ell,\ell')$ gives the force on the ℓth ion in the αth direction due to a unit displacement of the ℓ'th ion in the β direction. The Hamiltonian is written with the potential energy expanded in a Taylor series to second order (harmonic approximation),

$$H = V_0 + \frac{1}{2}\sum_{\ell\alpha} M\dot{u}_{\alpha}^2(\ell) + \frac{1}{2}\sum_{\substack{\alpha\beta \\ \ell,\ell'}} \frac{\partial^2 V}{\partial R_{\alpha}(\ell)\partial R_{\beta}(\ell')} u_{\alpha}(\ell)u_{\beta}(\ell') \quad , \tag{1.2}$$

and the derivatives are evaluated with all atoms at their equilibrium positions R_{ℓ}^0. This expression allows us to conveniently define the force constants as the second partial derivative of the effective ion-ion potential,

$$\Phi_{\alpha\beta}(\ell,\ell') = \frac{\partial^2 V}{\partial u_{\alpha}(\ell)\partial u_{\beta}(\ell')}\bigg|_0 \quad , \tag{1.3}$$

where $R(\ell) = R_{\ell}^0 + u(\ell)$ and it must be remembered that $R(\ell)$ and $u(\ell)$ have a time dependence which will become explicit shortly. From equation (1.3) and considerations of symmetry we have for a perfect lattice,

$$\Phi_{\alpha\beta}(\ell,\ell') = \Phi_{\beta\alpha}(\ell',\ell) \quad \text{and} \quad \Phi_{\alpha\beta}(\ell,\ell') = \Phi_{\alpha\beta}(m;0) \quad , \tag{1.4}$$

where $m = \ell - \ell'$.

Clearly the motion of the ℓth ion described by equation (1.1) is coupled to the displacement of all other ions. We assume a solution of the following form,

$$\underset{\sim}{u}(\ell,t) = \sum_{\underset{\sim}{k},\lambda} \frac{1}{M} \underset{\sim}{\varepsilon}(\underset{\sim}{k};\lambda) e^{i[\underset{\sim}{k}.\underset{\sim}{R}^0_\ell - \omega(\underset{\sim}{k};\lambda)t]} , \qquad (1.5)$$

where the time dependence appears explicitly and $\underset{\sim}{k}$ is any point in the FBZ. The vector $\underset{\sim}{\varepsilon}(\underset{\sim}{k};\lambda)$ is the phonon polarization vector (eigenfunction) and $\omega(\underset{\sim}{k},\lambda)$ is the corresponding normal mode (eigenfrequency) at the point $\underset{\sim}{k}$ in the FBZ. This solution effectively decouples equation (1.1). By inserting equation (1.5) into (1.1), using equations (1.4), and multiplying each side of the result by $e^{-i\underset{\sim}{k}.\underset{\sim}{R}^0_\ell}$ we are able to write,

$$\omega^2(\underset{\sim}{k};\lambda)\underset{\sim}{\varepsilon}_\alpha(\underset{\sim}{k};\lambda) = \sum_\beta [\frac{1}{M} \sum_{\ell'} e^{-i\underset{\sim}{k}.\underset{\sim}{R}^0_\ell} \Phi_{\alpha\beta}(m;0) e^{i\underset{\sim}{k}.\underset{\sim}{R}^0_{\ell'}}] \underset{\sim}{\varepsilon}_\beta(\underset{\sim}{k};\lambda) . \qquad (1.6)$$

The expression in square brackets in this equation does not depend on ℓ and ℓ' but rather on m and $\underset{\sim}{k}$. We, therefore, define the quantity

$$D_{\alpha\beta}(\underset{\sim}{k}) = \frac{1}{M} \sum_m e^{-i\underset{\sim}{k}.\underset{\sim}{R}^0_m} \Phi_{\alpha\beta}(m;0) , \qquad (1.7)$$

which is a function of $\underset{\sim}{k}$ in the FBZ and is called the dynamical matrix. It can be readily calculated in terms of force constants which, as has been pointed out, are

obtainable using the Born-von Kármán model. Combining equations (1.6) and (1.7), we have,

$$\omega^2(\underset{\sim}{k};\lambda)\underset{\sim}{\varepsilon}_\alpha(\underset{\sim}{k};\lambda) = \sum_\beta D_{\alpha\beta}(\underset{\sim}{k})\underset{\sim}{\varepsilon}_\beta(\underset{\sim}{k};\lambda) \quad . \tag{1.8}$$

In the alkalis this equation reduces to the simple eigenvalue problem of diagonalizing the 3×3 hermitian matrix $D_{\alpha\beta}(\underset{\sim}{k})$ at n points $\underset{\sim}{k}$ in the FBZ. This procedure yields the eigenvalues $\omega(\underset{\sim}{k};\lambda)$ and eigenfunctions $\underset{\sim}{\varepsilon}(\underset{\sim}{k};\lambda)$ that we have previously introduced.

We now wish to consider the electron phonon interaction. Following Carbotte and Dynes (1968) the potential energy of an electron at the point $\underset{\sim}{r}$ an a lattice can be written,

$$W(\underset{\sim}{r}) = \sum_\ell w(\underset{\sim}{r} - \underset{\sim}{R}_\ell) \quad , \tag{1.9}$$

where w is the electron-ion pseudopotential. The one orthogonal plane wave (OPW) approximation is assumed, (justification is offered in Chapter II), and the scattering of an electron from state $|\underset{\sim}{k}\rangle$ to $|\underset{\sim}{k}+\underset{\sim}{q}\rangle$ is described by the matrix element,

$$\langle \underset{\sim}{k}+\underset{\sim}{q}|W(\underset{\sim}{r})|\underset{\sim}{k}\rangle = \frac{1}{V}\int e^{-i(\underset{\sim}{k}+\underset{\sim}{q})\cdot\underset{\sim}{r}} \sum_\ell w(\underset{\sim}{r}-\underset{\sim}{R}_\ell) e^{i\underset{\sim}{k}\cdot\underset{\sim}{r}} d^3\underset{\sim}{r} \quad , \tag{1.10}$$

where V is the total crystal volume. Following the treatment

of Trofimenkoff (1969) we define a static structure factor,

$$S(\underset{\sim}{q}) \equiv \frac{1}{N} \sum_{\ell} e^{-i\underset{\sim}{q}.\underset{\sim}{R}(\ell)} \quad , \tag{1.11}$$

and then rewrite equation (1.10) in the more convenient form

$$\langle \underset{\sim}{k}+\underset{\sim}{q} | W(\underset{\sim}{r}) | \underset{\sim}{k} \rangle = S(\underset{\sim}{q}) \langle \underset{\sim}{k}+\underset{\sim}{q} | w(\underset{\sim}{r}) | \underset{\sim}{k} \rangle \quad , \tag{1.12}$$

where,

$$\langle \underset{\sim}{k}+\underset{\sim}{q} | w(\underset{\sim}{r}) | \underset{\sim}{k} \rangle = w(\underset{\sim}{q}) = \frac{1}{\Omega_0} \int e^{-i(\underset{\sim}{k}+\underset{\sim}{q}).\underset{\sim}{r}} w(\underset{\sim}{r}) e^{i\underset{\sim}{k}.\underset{\sim}{r}} d^3\underset{\sim}{r} \ , \tag{1.13}$$

is the pseudopotential form factor. Since in the one OPW approximation we only consider scattering on the Fermi surface, the matrix element is only a function of momentum transfer. The maximum momentum transfer allowed is, therefore, $2k_F$, the diameter of the Fermi sphere.

For small displacements the structure factor can be expanded to first order to obtain the electron phonon contribution to the hamiltonian,

$$S(\underset{\sim}{q}) = \frac{1}{N} \sum_{\ell} e^{-i\underset{\sim}{q}.(\underset{\sim}{R}^0_\ell + \underset{\sim}{u}_\ell)} \approx \frac{1}{N} \sum_{\ell} e^{-i\underset{\sim}{q}.\underset{\sim}{R}^0_\ell} \{1 - i\underset{\sim}{q}.\underset{\sim}{u}_\ell\} \quad , \tag{1.14}$$

where the abbreviated notation $\underset{\sim}{u}_\ell$ has been adopted in place of $\underset{\sim}{u}(\ell)$. It is convenient at this point to introduce the electron-ion hamiltonian in second quantized notation,

$$H_{el\text{-}ion} = \sum_{\underset{\sim}{q},\underset{\sim}{k},\sigma} \langle \underset{\sim}{k}+\underset{\sim}{q}|W(\underset{\sim}{r})|\underset{\sim}{k}\rangle C^{\dagger}_{\underset{\sim}{k}+\underset{\sim}{q};\sigma} C_{\underset{\sim}{k};\sigma} \tag{1.15}$$

where $C^{\dagger}_{\underset{\sim}{k}+\underset{\sim}{q};\sigma}$ and $C_{\underset{\sim}{k};\sigma}$ are the electron creation and annihilation operators, respectively, which describe transition from state $|\underset{\sim}{k}\rangle$ to $|\underset{\sim}{k}+\underset{\sim}{q}\rangle$ with spin σ. Equations (1.12) and (1.14) are now substituted into equation (1.15) to yield,

$$H_{el\text{-}ph} = \sum_{\underset{\sim}{q},\underset{\sim}{k},\sigma} \frac{1}{N} \sum_{\ell} - i\underset{\sim}{q}.\underset{\sim}{u}_{\ell} \langle \underset{\sim}{k}+\underset{\sim}{q}|w(\underset{\sim}{r})|\underset{\sim}{k}\rangle e^{-i\underset{\sim}{q}.\underset{\sim}{R}^{0}_{\ell}}$$

$$\times C^{\dagger}_{\underset{\sim}{k}+\underset{\sim}{q};\sigma} C_{\underset{\sim}{k};\sigma} \quad , \tag{1.16}$$

where the contribution of the first term of equation (1.14), (which leads to the equilibrium energy), has been dropped. We are left with the hamiltonian for the electron phonon interaction.

To further reduce the expression for $H_{el\text{-}ph}$ we expand the excursions from equilibrium $\underset{\sim}{u}_{\ell}$ in terms of normal coordinates $Q(\underset{\sim}{k}';\lambda)$,

$$\underset{\sim}{u}_{\ell} = \frac{1}{\sqrt{MN}} \sum_{\underset{\sim}{k}';\lambda} Q(\underset{\sim}{k}';\lambda)\underset{\sim}{\varepsilon}(\underset{\sim}{k}';\lambda) e^{i\underset{\sim}{k}'.\underset{\sim}{R}^{0}_{\ell}} \quad , \tag{1.17}$$

where the sum over $\underset{\sim}{k}'$ extends over the FBZ and M is the ion mass. It is important at this point to appreciate the importance of the expression,

$$\frac{1}{N}\sum_{\ell} e^{-i(\underset{\sim}{q}-\underset{\sim}{k}').\underset{\sim}{R}^0_\ell} = \delta_{\underset{\sim}{k}'-\underset{\sim}{q},\underset{\sim}{\kappa}_n} \quad , \tag{1.18}$$

where $\underset{\sim}{\kappa}_n$ is a reciprocal lattice vector. As the sum over $\underset{\sim}{k}'$ is performed in equation (1.17) and $\underset{\sim}{k}'$ sweeps the FBZ, the Kronecker delta will be non-zero for only one value of $\underset{\sim}{k}'$: the value for which $\underset{\sim}{\kappa}_n + \underset{\sim}{q} = \underset{\sim}{k}'$ is in the FBZ. We can, therefore, formally replace $\underset{\sim}{k}'$ by $\underset{\sim}{q}$ since the phonons are completely described in the FBZ and $\underset{\sim}{q}$ is read as reduced to the FBZ. This applies to the arguments of both the normal coordinates $Q(\underset{\sim}{q},\lambda)$ and the polarization vectors $\underset{\sim}{\varepsilon}(\underset{\sim}{q};\lambda)$.

By expanding the normal coordinates in terms of phonon creation and annihilation operators,

$$Q(\underset{\sim}{k};\lambda) = [2\omega(\underset{\sim}{k};\lambda)]^{-1/2}(a^{\dagger}_{-\underset{\sim}{k};\lambda} + a_{\underset{\sim}{k};\lambda}) \quad , \tag{1.19}$$

and using equations (1.16), (1.17) and (1.18) we can write the electron phonon interaction hamiltonian as,

$$H_{el\text{-}ph} = \sum_{\underset{\sim}{k},\underset{\sim}{q};\sigma,\lambda} g_{\underset{\sim}{k}+\underset{\sim}{q},\underset{\sim}{k};\lambda}\, c^{\dagger}_{\underset{\sim}{k}+\underset{\sim}{q};\sigma} c_{\underset{\sim}{k}\sigma}(a^{\dagger}_{-\underset{\sim}{q}\lambda} + a_{\underset{\sim}{q}\lambda}) \tag{1.20}$$

where the electron phonon coupling constant is defined by,

$$g_{\underset{\sim}{k}+\underset{\sim}{q},\underset{\sim}{k};\lambda} \equiv -i\left[\frac{\hbar}{2MN\omega(\underset{\sim}{q};\lambda)}\right]^{1/2} \underset{\sim}{q}.\underset{\sim}{\varepsilon}(\underset{\sim}{q};\lambda)\langle \underset{\sim}{k}+\underset{\sim}{q}|w(\underset{\sim}{r})|\underset{\sim}{k}\rangle \quad . \tag{1.21}$$

From equation (1.20) it is clear that g is the scattering amplitude for phonon mediated scattering of electrons from

state $|\underset{\sim}{k}>$ to state $|\underset{\sim}{k}+\underset{\sim}{q}>$ on the Fermi surface.

We have thus far considered the theory of phonons and the electron phonon interaction. We now apply this information to construct phonon frequency distributions. These weighted frequency distributions will be useful in the calculations of transport properties in the alkalis.

Following Carbotte and Dynes (1968) the phonon density of states can be written,

$$F(\omega) = \frac{1}{N} \sum_{\lambda} \int \frac{d^3q}{(2\pi)^3} \delta(\omega - \omega(\underset{\sim}{q};\lambda)) \quad , \tag{1.22}$$

where the integral is restricted to the FBZ. From a knowledge of the $\omega(\underset{\sim}{q};\lambda)$ gained by diagonalizing the dynamical matrix throughout the FBZ, we can construct a histogram of phonon frequencies and thus obtain an approximate phonon frequency distribution or density of phonon states.

A distribution arising in superconductivity which is closely related to the phonon density of states can be defined as,

$$\alpha^2(\omega)F(\omega) = \frac{\sum_{\lambda} \int_{S_F} d^2\underset{\sim}{k} \int_{S_F'} d^2\underset{\sim}{k}' \frac{|g_{\underset{\sim}{k},\underset{\sim}{k}';\lambda}|^2}{(2\pi)^3 v_F} \delta(\omega-\omega(\underset{\sim}{k}-\underset{\sim}{k}';\lambda))}{\int_{S_F} d^2\underset{\sim}{k}} , \tag{1.23}$$

where v_F is the Fermi velocity and the integrals are over the Fermi surface. Since it is assumed that the Fermi surface is spherical and that the coupling constant g depends only on momentum transfer, we can reduce the two surface integrals to a three-dimensional integral over momentum transfer, $\underset{\sim}{q}$. The expression can, therefore, be written in the more convenient form,

$$\alpha^2(\omega)F(\omega) = \frac{1}{N}\sum_{\lambda}\int_{<2k_F}\frac{d^3q}{(2\pi)^3}L_\lambda(\underset{\sim}{q})\delta(\omega - \omega(\underset{\sim}{q};\lambda)) \quad , \tag{1.24}$$

where the integral extends throughout a sphere of radius $2k_F$ and the weighting factor is given by,

$$L_\lambda(\underset{\sim}{q}) = \frac{1}{4}\frac{m}{M}\frac{|\underset{\sim}{q}.\underset{\sim}{\varepsilon}(\underset{\sim}{q};\lambda)|^2|w(\underset{\sim}{q})|^2}{k_F\, q\, \omega(\underset{\sim}{q};\lambda)} \quad . \tag{1.25}$$

In equation (1.25) m is the electron mass and M is the ionic mass. The similarity between equations (1.22) and (1.24) suggests that the two distributions can be calculated in a similar manner. This is in fact the case although in equation (1.24) the integration must be performed throughout a sphere of radius $2k_F$ rather than simply throughout the FBZ. The weighting factor, equation (1.25), can be calculated readily since we obtain both the eigenfrequencies $\omega(\underset{\sim}{q};\lambda)$ and the eigenfunctions $\underset{\sim}{\varepsilon}(\underset{\sim}{q};\lambda)$ from the diagonalization of the dynamical matrix within the FBZ or in the case of equation (1.24), throughout a sphere of radius $2k_F$.

From calculations of transport properties we can define another phonon frequency distribution,

$$\alpha^2_{tr}(\omega)F(\omega) = \frac{1}{N}\sum_{\lambda}\int \frac{d^3q}{(2\pi)^3}\frac{q^2}{2k_F^2} L_{\lambda}(\underset{\sim}{q})\delta(\omega - \omega(\underset{\sim}{q};\lambda)) \quad . \tag{1.26}$$

It contains the additional weighting factor $q^2/2k_F^2$ corresponding to $(1 - \cos\theta)$. The contribution of this factor is apparent when one considers the importance of large angle scattering in transport properties such as resistivity. In a manner similar to $F(\omega)$ and $\alpha^2(\omega)F(\omega)$ this distribution can be readily calculated on the basis of the theory considered in this section.

1.2 Numerical Techniques

Now that the theory has been considered we turn our attention to the numerical techniques employed to calculate phonon frequency distribution functions. Gilat and Dolling (1964) and Gilat and Raubenheimer (1966) have developed a computer programme which calculates the phonon density of states $F(\omega)$. They employ a numerical extrapolation technique which greatly increases the sampling size and hence the frequency resolution without unduely increasing the computation time. Their technique which applies to the FBZ for $F(\omega)$ has been generalized by Carbotte and Dynes (1968) to sample beyond the FBZ to a radius of $2k_F$ and to include a weighting factor proportional to the electron phonon coupling constant. This allows calculation of $\alpha^2(\omega)F(\omega)$ and other frequency distributions to a high degree of accuracy.

The computer programme itself is described in some detail in Appendix A. The discussion which follows in this Section will, therefore, be concerned with the theory behind the numerical methods.

For cubic crystals, symmetry considerations allow us to restrict our attention to a 1/48 irreducible sector of the FBZ. This in itself affords great saving in computation, for in essence our task is that of solving the dynamical

matrix $D_{\alpha\beta}(\underset{\sim}{q})$ at all points $\underset{\sim}{q}$ in the FBZ. At least this is the case for $F(\omega)$. In calculating $\alpha^2(\omega)F(\omega)$ and similar distributions, it can be seen from equation (1.25) that the weighting factor has a significant $\underset{\sim}{q}$ dependence. Since we wish to consider umklapp processes we must extend our sampling of $\underset{\sim}{q}$ in the Brillouin Zone (BZ) to include all points within a sphere of radius $2k_F$. Dynes (1968) achieves this end by recognizing the repeatability of the dispersion curves in the second zone and beyond. He constructs a set of coordinate transformations which define points $\underset{\sim}{q}$ in an extension of the 1/48 irreducible sector beyond the FBZ boundary and less than $2k_F$, in terms of points in the corresponding FBZ. Hence it is possible to obtain solutions for $D_{\alpha\beta}(\underset{\sim}{q})$ to radius $2k_F$ in the BZ by solving the $D_{\alpha\beta}(\underset{\sim}{q})$ only within the 1/48 irreducible sector of the FBZ and carrying out the relevant transformations. This transformation technique contributes to a considerable reduction in calculation time since matrix diagonalization is the slowest part of the computation.

We are left then with the problem of diagonalizing the $D_{\alpha\beta}(\underset{\sim}{q})$ in the 1/48 irreducible sector of the FBZ. This is accomplished very efficiently using the extrapolation method which effectively extracts "all" frequencies and requires only a minimum number of diagonalizations.

Previously we have demonstrated that the dynamical matrix $D^0_{\alpha\beta}(\underset{\sim}{q})$ can be obtained from a knowledge of the force

constants, equation (1.7). Using a slightly modified notation we write the corresponding secular equation,

$$|D^0_{\alpha\beta}(\underset{\sim}{q}) - \omega_0^2(\underset{\sim}{q};\lambda)\delta_{\alpha\beta}| = 0 \quad . \tag{1.27}$$

Diagonalization of $D^0_{\alpha\beta}(\underset{\sim}{q})$ results in a diagonal matrix $\Lambda^0_{\lambda\lambda}(\underset{\sim}{q})$ satisfying

$$\Lambda^0_{\lambda\lambda}(\underset{\sim}{q}) = \omega_0^2(\underset{\sim}{q};\lambda) \quad , \tag{1.28}$$

where

$$U^\dagger(\underset{\sim}{q})D^0(\underset{\sim}{q})U(\underset{\sim}{q}) = \Lambda^0(\underset{\sim}{q}) \quad , \tag{1.29}$$

and $U(\underset{\sim}{q})$ is a unitary matrix which diagonalizes $D^0(\underset{\sim}{q})$. Extrapolation is carried out by solving for eigenvalues $\omega_0(\underset{\sim}{q};\lambda)$ at evenly spaced points in the FBZ and then establishing other eigenvalues by taylor expanding about these intermediate points. The $\underset{\sim}{q}$'s are chosen sufficiently close together that linear extrapolation is a good approximation.

The expansion is obtained by calculating the gradient of phonon frequency $\omega(\underset{\sim}{q};\lambda)$ and this is accomplished in the following way. First, we establish modified dynamical matrices $D^\gamma(\underset{\sim}{q} + \hat{e}_\gamma \delta q_\gamma)$ where $\hat{e}_\gamma$ is a unit vector along the γth cartesian axis and δq_γ is a small increment in the same direction. The difference matrix is formed,

$$\Delta^{\gamma}_{\alpha\beta}(\underset{\sim}{q}) = D^{\gamma}_{\alpha\beta}(\underset{\sim}{q} + \hat{e}_{\gamma}\delta q_{\gamma}) - D^{0}_{\alpha\beta}(\underset{\sim}{q}) \quad , \tag{1.30}$$

and perturbation theory is employed to obtain $\eta^{\gamma}_{\lambda} \equiv \delta(\omega_0^2(\underset{\sim}{q};\lambda)$, the change in the λth eigenvalue of $D^0(\underset{\sim}{q})$. We have

$$\eta^{\gamma}_{\lambda} \approx \Delta'^{\gamma}_{\lambda\lambda} + \sum_{\lambda\neq\lambda'} \frac{(\Delta'^{\gamma}_{\lambda\lambda'})^2}{\Lambda^0_{\lambda'\lambda'} - \Lambda^0_{\lambda\lambda}} \quad , \tag{1.31}$$

where

$$\Delta'^{\gamma}_{\lambda\lambda'}(\underset{\sim}{q}) = \{U^{\dagger}(\underset{\sim}{q})\Delta^{\gamma}(\underset{\sim}{q})U(\underset{\sim}{q})\}_{\lambda\lambda'} \quad .$$

Gilat and Dolling (1964) point out that higher order terms are small so only the first term in equation (1.31) is retained. Using this fact and the definition of η^{γ}_{λ}, we can write,

$$[\nabla_{\underset{\sim}{q}}\omega(\underset{\sim}{q};\lambda)]_{\gamma} \approx \frac{1}{2\omega_0(\underset{\sim}{q};\lambda)} \cdot \frac{\Delta'^{\gamma}_{\lambda\lambda}(\underset{\sim}{q})}{\delta q_{\gamma}} \quad , \tag{1.32}$$

so we now have a convenient method of calculating the gradient of $\omega(\underset{\sim}{q};\lambda)$. The phonon frequencies at these intermediate points will, therefore, be

$$\omega(\underset{\sim}{q} + \Delta\underset{\sim}{q};\lambda) = \omega_0(\underset{\sim}{q};\lambda) + \nabla_{\underset{\sim}{q}}\omega(\underset{\sim}{q};\lambda).\Delta\underset{\sim}{q} \quad . \tag{1.33}$$

The extrapolation method is actually applied by considering the FBZ divided into a uniform simple cubic mesh of points $\underset{\sim}{q}_c$, separated by a constant distance. Each

$\underset{\sim}{q}_c$ is considered to be at the center of a small cube throughout which extrapolation is carried out at a finite number of points. The cubes are small enough that linearity is a reasonable assumption.

It is possible to consider a constant frequency surface associated with each intermediate point $\underset{\sim}{q}$ in the cube. The number of frequencies between $\omega_0(\underset{\sim}{q}_c;\lambda)$ and $\omega_0(\underset{\sim}{q}_c;\lambda) + d\omega$ is, therefore, proportional to the volume element contained between the two constant frequency surfaces. The contribution of all frequencies $\omega(\underset{\sim}{q};\lambda)$ is, therefore, taken into consideration in constructing the frequency histogram.

In practice the mesh of points $\underset{\sim}{q}_c$ is divided up into five regions and the spacing decreases from region to region as one approaches the origin. This is necessary since a finer mesh is required to adequately represent the acoustic modes near $q = 0$. Some of the cubes will lie on the boundary of the 1/48 irreducible sector. They are, therefore, weighted somewhat differently from those cubes which lie in the middle of the sector. In establishing suitable mesh spacings Dynes and Carbotte (1968) systematically reduced the spacing until stable results for a resistivity calculation were obtained.

The basic techniques described in this Chapter have been rigorously tested in the earlier $F(\omega)$ programme of Gilat and Raubenheimer (1966), and their results agree

closely with experiment. A further indication of the validity of the methods is that Van Hove singularities in the frequency distributions are clearly resolved. This can be seen in Fig. 1.1 where phonon frequency distributions for potassium are displayed.

Fig. 1.1 Frequency distributions for Potassium

$F(\nu)$ ———

$\alpha^2_{tr}(\nu)F(\nu)$ . . .

$\alpha^2(\nu)F(\nu)$ - - -

Note: $\alpha^2_{tr}(\nu)F(\nu)$ and $\alpha^2(\nu)F(\nu)$ have been scaled up by a factor of 10.

Fig. 1.1

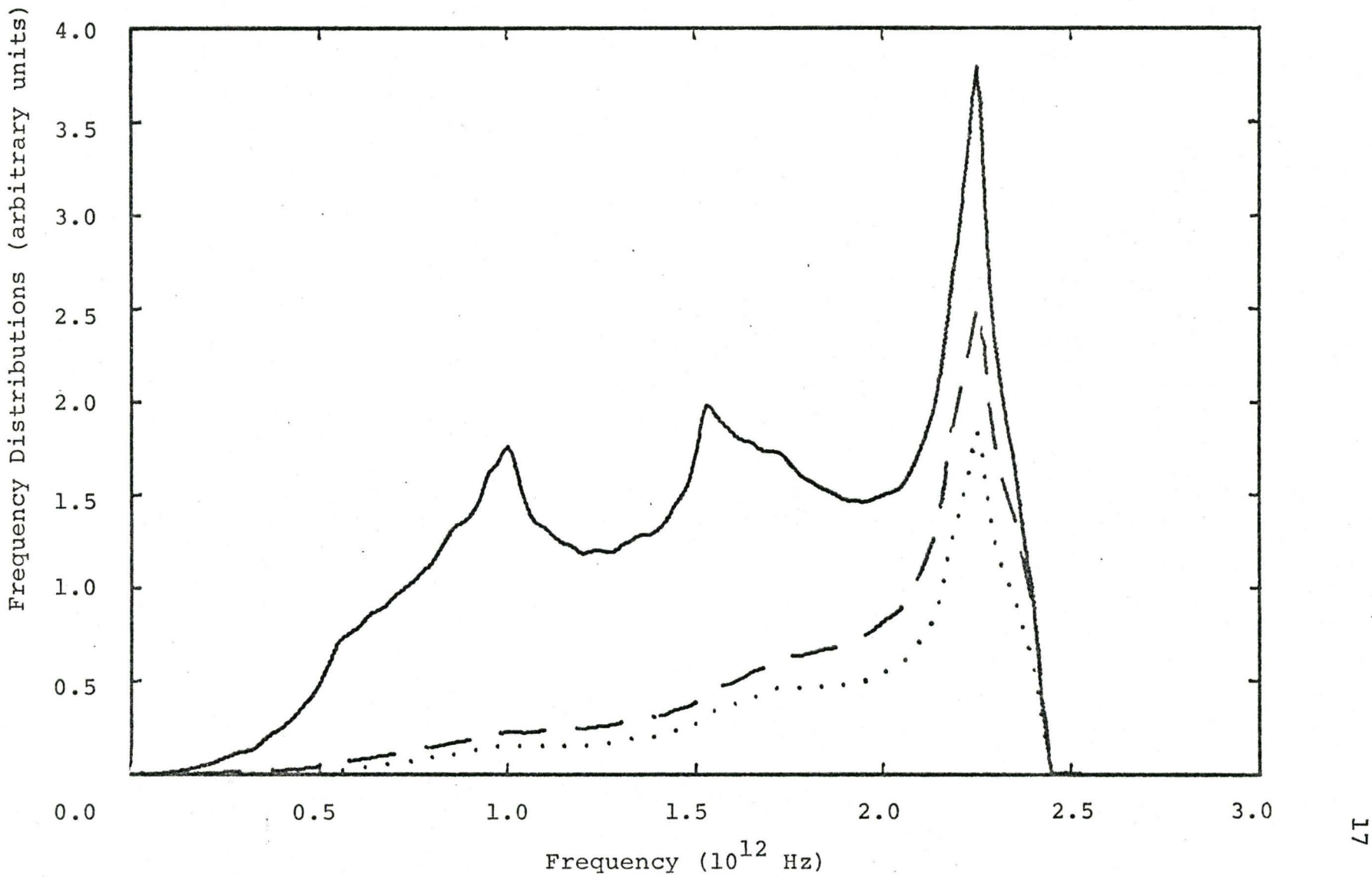
Frequency Distributions (arbitrary units)
4.0
3.5
3.0
2.5
2.0
1.5
1.0
0.5
0.0
0.5
1.0
1.5
2.0
2.5
3.0
Frequency (10^{12} Hz)

CHAPTER II

SCREENING THE ASHCROFT PSEUDOPOTENTIAL

2.1 General Theory

For the alkalis it is possible to consider the electrons in two groups; those in nonlocal conduction states and those localized in core states. The two separate states are orthogonal by the exclusion principle. Because electrons in the alkalis can be considered in this way we are able to apply pseudopotential theory to describe the interaction of electrons with the lattice.

In essence, use of the pseudopotential method allows us to transform the problem of electrons in conduction states interacting with ions so that the mathematical treatment is simpler. Instead of dealing with real conduction electron wave functions in a real interionic potential, we make a transformation and solve instead an equivalent but simpler problem. We consider pseudoelectron wave functions of orthogonal plane waves (OPW) in a pseudopotential. The result is applicable to our original and mathematically more complicated problem.

One can express this orthogonalization between core and conduction electron states as an extra repulsive term added to the original attractive electron ion potential.

Both terms act on the pseudoelectron wave function and the resulting cancellation between attractive and repulsive terms yields a weak pseudopotential. The pseudoelectron wave function may, therefore, be expanded in a small number of OPWs. This justifies the assumption that a one OPW approximation is adequate for the alkalis.

From pseudopotential theory we are able to derive the matrix element for scattering from state $|\underset{\sim}{k}\rangle$ to state $|\underset{\sim}{k}+\underset{\sim}{q}\rangle$ and we can write,

$$w^0(\underset{\sim}{q}) = \langle \underset{\sim}{k}+\underset{\sim}{q}|w^0(\underset{\sim}{r})|\underset{\sim}{k}\rangle \quad . \tag{2.1}$$

Here we have employed the local approximation so that the bare pseudopotential $w^0(q)$ is a function of momentum transfer only. Equation (2.1) describes the bare pseudopotential associated with each ion.

For the purpose of this discussion we restrict ourselves to the Ashcroft pseudopotential as it has been found to give a satisfactory description of the properties of the alkalis, Hayman and Carbotte (1971). It can be written as an effective potential,

$$\begin{aligned} V_{eff}(\underset{\sim}{r}) &= \frac{-Ze^2}{r} \quad ; \quad r > R_c \quad , \\ V_{eff}(\underset{\sim}{r}) &\approx 0 \quad ; \quad r < R_c \quad . \end{aligned} \tag{2.2}$$

The parameter R_c is adjustable and is expected to be close to the usual ionic radius. In the region $r < R_c$ the core states are orthogonal to the plane wave like conduction electron states and the net effect is a cancellation leaving the weak pseudopotential. In momentum representation we employ the analytic form,

$$w^0(\underset{\sim}{q}) = \frac{-4\pi Ze^2}{\Omega^0 q^2} \cos(q\ R_c\ a) \quad , \tag{2.3}$$

where Ω^0 is the ionic volume and a is the lattice parameter. The adjustable parameter R_c is established by fitting to electrical resistivity data at 100K.

In practice the pseudopotential seen by a conduction electron in an OPW state is modified or screened by the presence of other conduction electrons. This effect is described by a dielectric function $\varepsilon^*(\underset{\sim}{q})$ which is not to be confused with the phonon polarization vector. The screened pseudopotential is written,

$$w(\underset{\sim}{q}) = \frac{w^0(\underset{\sim}{q})}{\varepsilon^*(\underset{\sim}{q})} \quad . \tag{2.4}$$

We now concentrate on the dielectric function although consideration is limited to two types. In general, the dielectric function can be written,

$$\varepsilon^*(\underset{\sim}{q}) = 1 + [1 - f(\underset{\sim}{q})] \frac{4\pi Ze^2}{\Omega_0 q^2} \left(\frac{2}{3} E_F\right)^{-1} F(q) \quad , \qquad (2.5)$$

where

$$F(q) = \frac{1}{2} + \frac{4k_F^2 - q^2}{8k_F q} \ln \left| \frac{2k_F + q}{2k_F - q} \right| \quad . \qquad (2.6)$$

The factor $f(\underset{\sim}{q})$ is an adjustable function which accounts for exchange and correlation effects. We consider two cases. The first of these ignores many body effects and we obtain the Hartree or Lindhard dielectric function by setting $f(q) = 0$.

Recently, Singwi et al. (1970), have constructed a factor by a self consistent method, which considers exchange and includes Coulomb correlation effects. The factor is incorporated in the dielectric function by making the substitution,

$$f(q) = A(1 - e^{-B(q/k_F)^2}) \quad . \qquad (2.7)$$

In this equation the constants A and B are weakly dependent on the density parameter r_S, which is defined by,

$$\frac{\Omega^0}{Z} = \frac{4\pi}{3} r_S^3 a_0^3 \quad , \qquad (2.8)$$

where a_0 is the Bohr radius. Parameters relevant to pseudopotential calculations are tabulated in Table (2.1), following Price et al. (1970). When the factor defined in

TABLE 2.1

PSEUDOPOTENTIAL PARAMETERS

	Li	Na	K	Rb
a_{Hayman}	3.4853	4.2268	5.2275	5.5855
a_{Singwi}	3.478	4.225	5.225	5.585
r_S	3.236	3.931	4.862	5.197
A	0.999	0.995	1.007	1.008
B	0.258	0.2625	0.249	0.247
$R_{c_{Hayman}}$	1.000353	0.8282	1.0353	1.0422
$R_{c_{Mason}}$	0.959	0.878	1.105	1.119

equation (2.7) is included in the dielectric function, the result will be referred to as the Singwi dielectric function.

2.2 Calculations and Results

Calculations of both Hartree and Singwi screened Ashcroft pseudopotentials have been made in order to assess the importance of including correlation and exchange. Figures (2.1) to (2.4) show the result of inclusion of many body effects in the dielectric functions of several alkalis. For the same value of R_c, the shape of the pseudopotential is changed significantly.

The values of R_c for the Hartree dielectric function were established by fitting to the electrical resistivity. When we fit the Singwi R_c in the same way the node is shifted. This is significant since transport properties are very much dependent on the position of the first node of the pseudopotential. If the node is less than $2k_F$, then significant contribution from umklapp processes is present. This is the case with lithium.

In Table (2.2) we compare electrical resistivities calculated using the different dielectric functions. It can be seen that for the same values of R_c, a change in the screening can have as much as a 40% effect on the resistivity.

Clearly the inclusion of correlation and exchange has a significant effect on the pseudopotential. It should be remembered, however, that the Ashcroft pseudopotential itself is very crude. Before complicated screening can be

Fig. 2.1 Ashcroft pseudopotentials for Lithium

Hartree Screening ———

R_c = 1.000353 a = 3.4853

Singwi Screening . . .

R_c = 1.000353 a = 3.4853

Singwi Screening - - -

R_c = 0.959 a = 3.478

Note: a is the lattice parameter.

Fig. 2.1

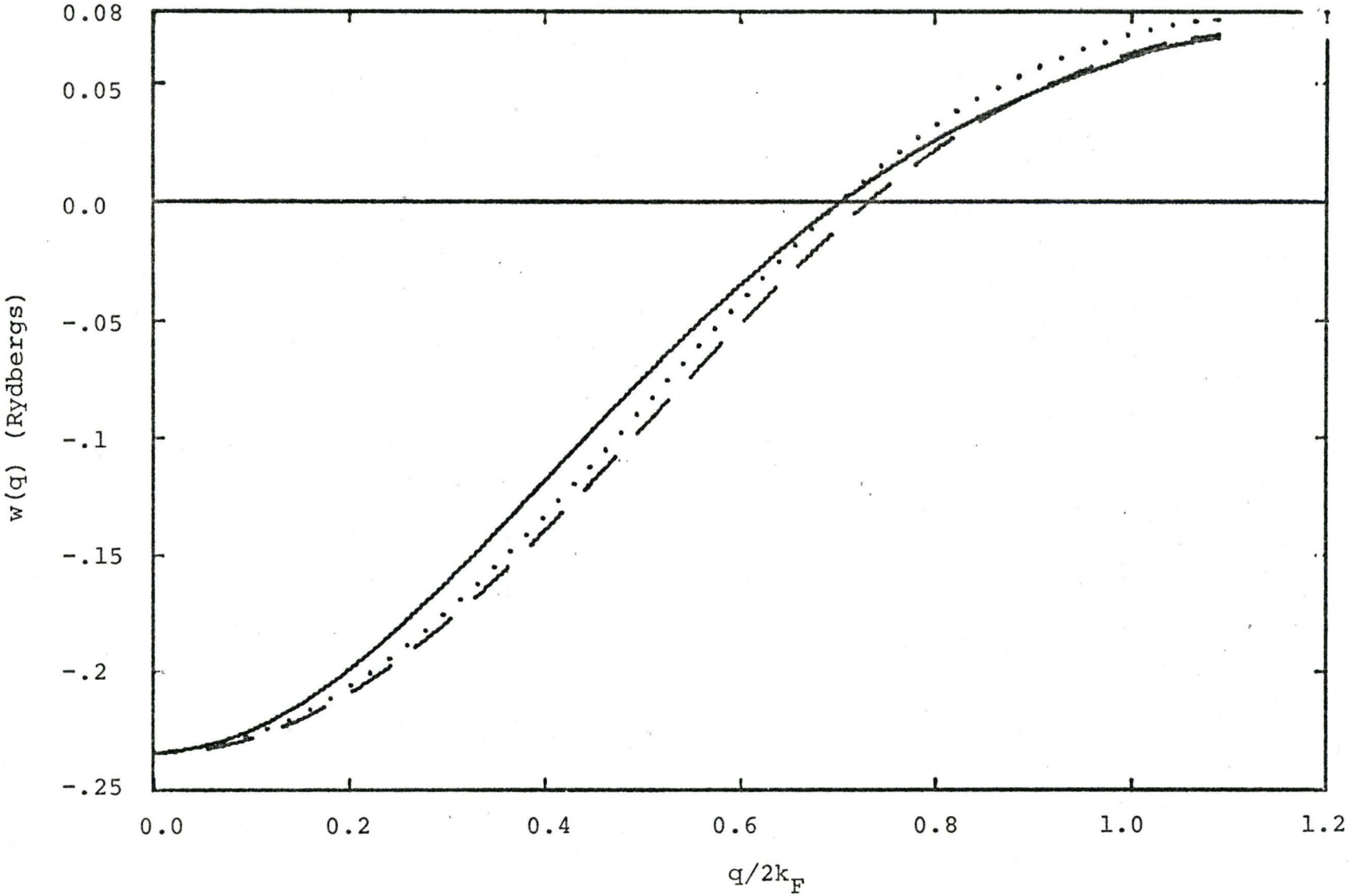

Fig. 2.2 Ashcroft pseudopotentials for Potassium

Hartree Screening ———

R_c = 1.0353 a = 5.2275

Singwi Screening . . .

R_c = 1.0353 a = 5.2275

Singwi Screening - - -

R_c = 1.105 a = 5.225

Note: a is the lattice parameter.

Fig. 2.2

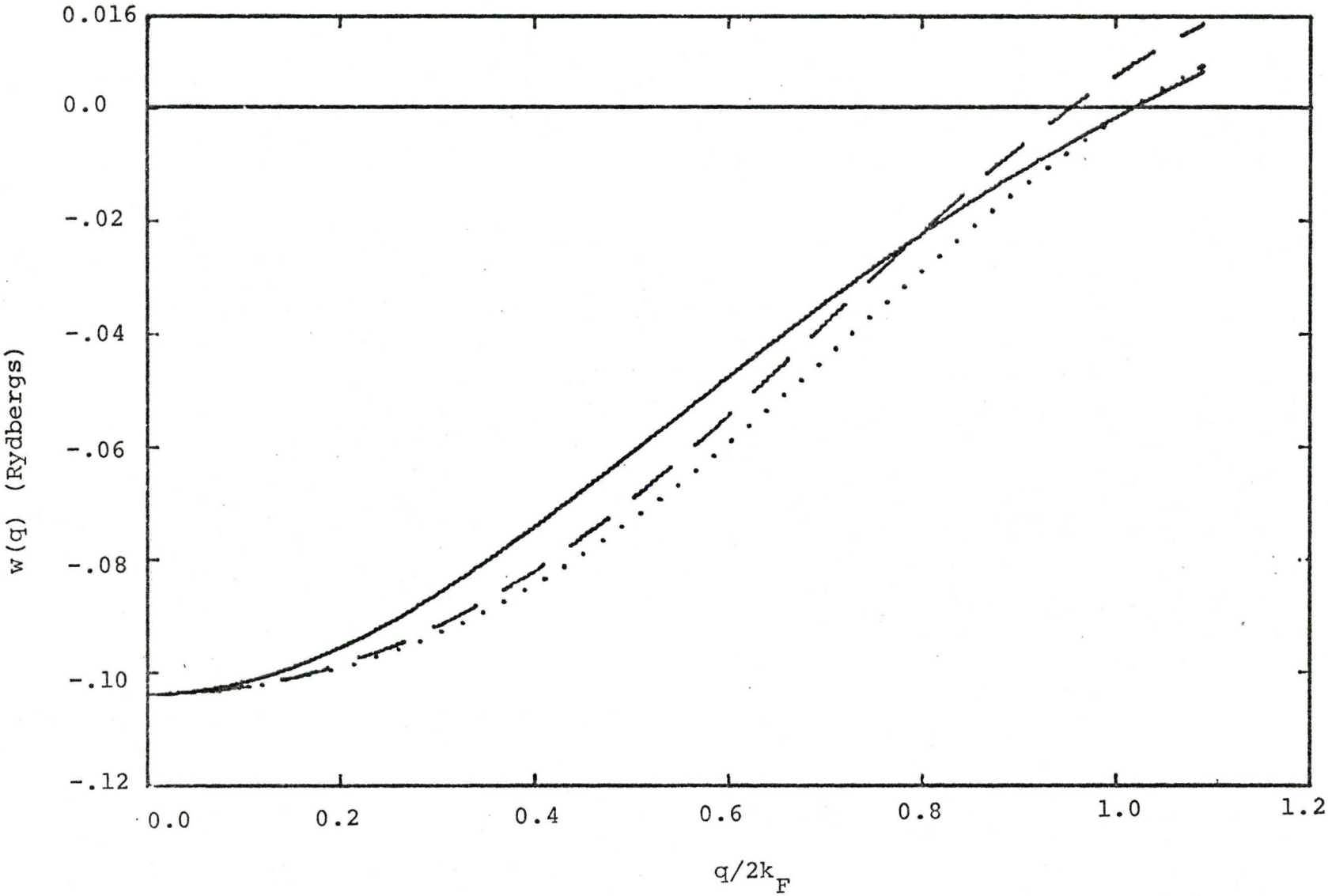

Fig. 2.3 Ashcroft pseudopotentials for Sodium

Hartree Screening ———

R_c = 0.8282 a = 4.2268

Singwi Screening . . .

R_c = 0.8282 a = 4.2268

Singwi Screening - - -

R_c = 0.878 a = 4.225

Note: a is the lattice parameter.

Fig. 2.3

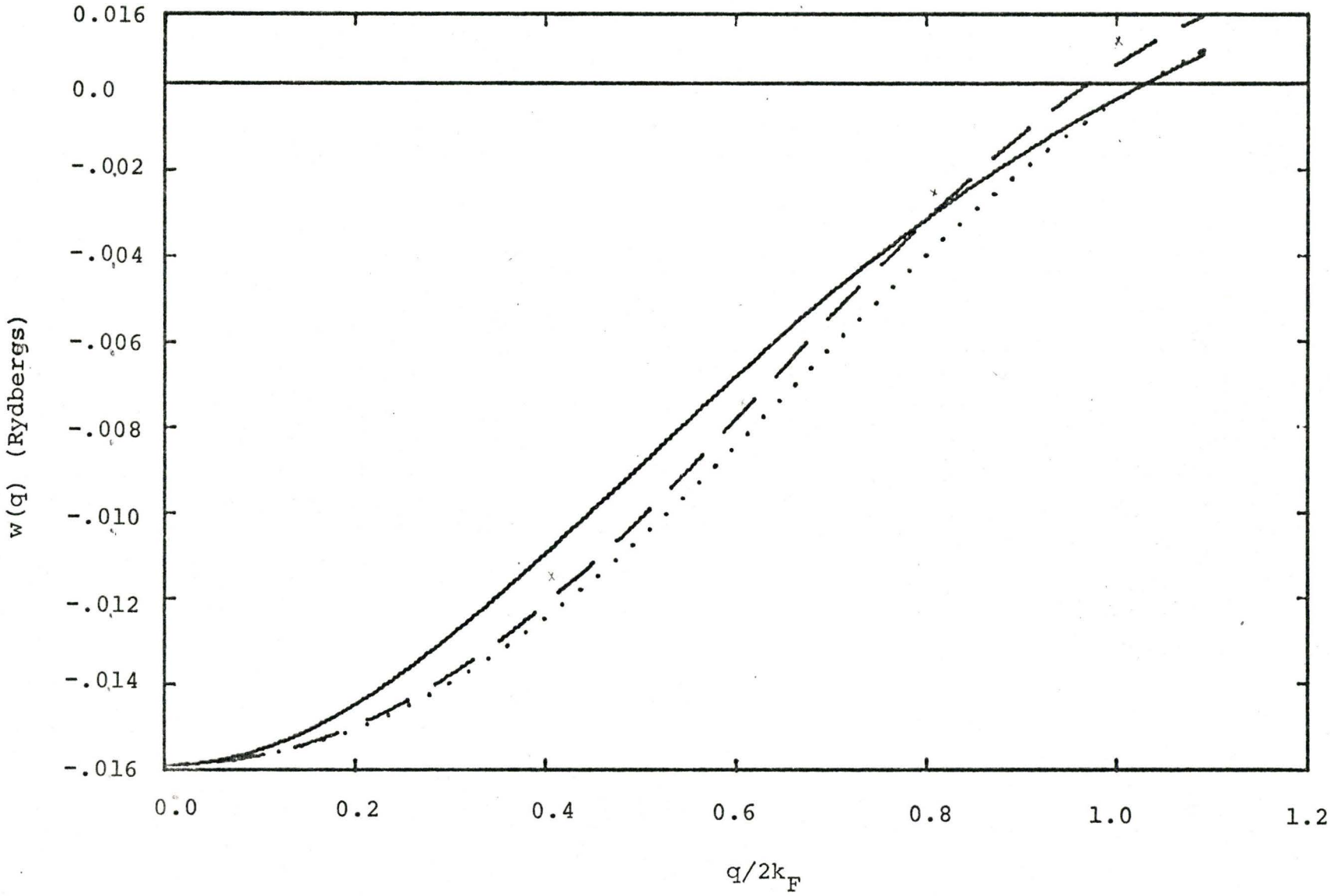
0.016
0.0
-.002
-.004
-.006
-.008
-.010
-.012
-.014
-.016
w(q) (Rydbergs)
0.0
0.2
0.4
0.6
0.8
1.0
1.2
q/2k_F

Fig. 2.4 Ashcroft pseudopotentials for Rubidium

Hartree Screening ———

R_c = 1.0422 a = 5.5855

Singwi Screening . . .

R_c = 1.0422 a = 5.5855

Singwi Screening - - -

R_c = 1.119 a = 5.585

Note: a is the lattice parameter.

Fig. 2.4

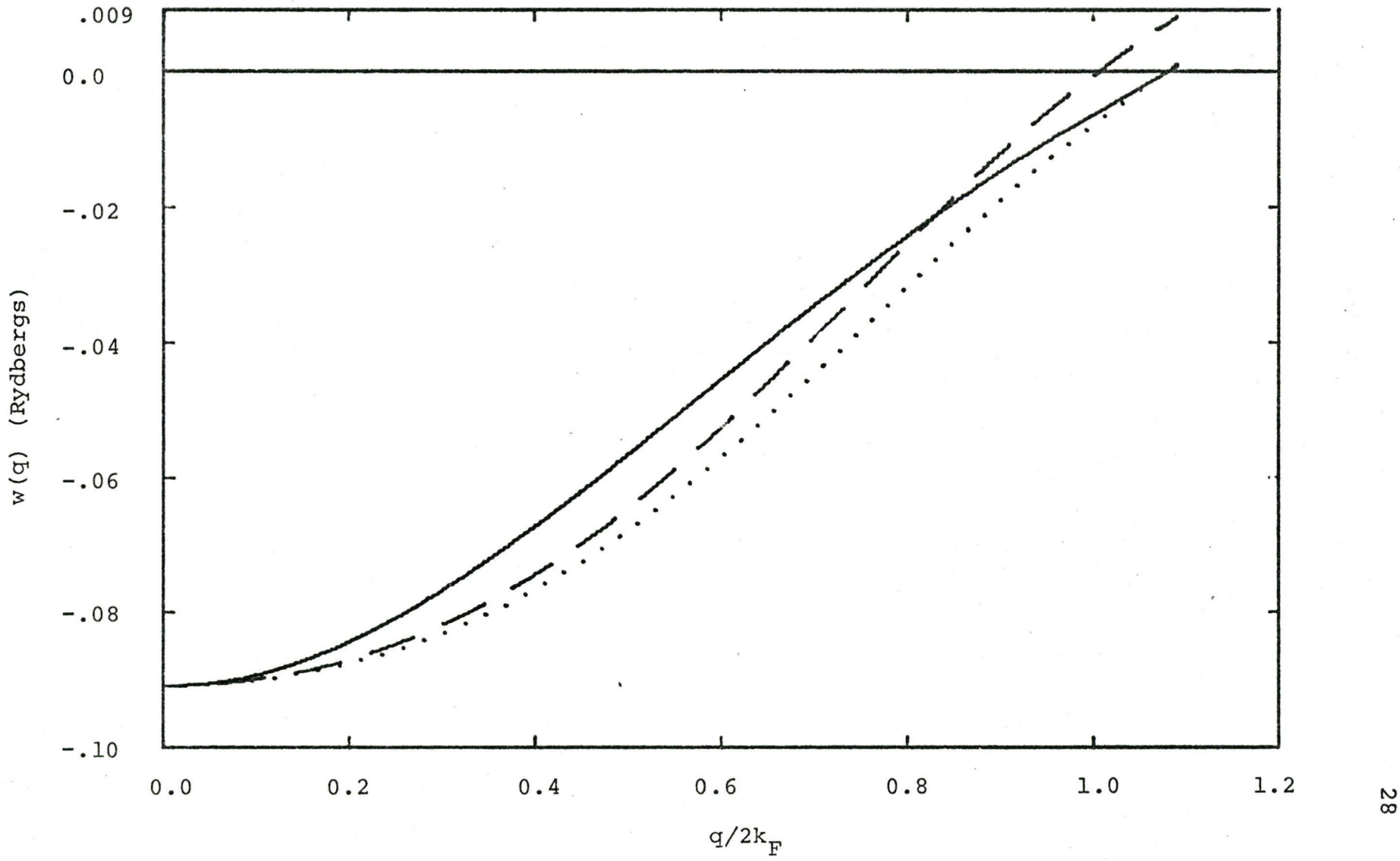

TABLE 2.2

ELECTRICAL RESISTIVITY $\rho(T)$ FOR SODIUM ($\mu\Omega$-cm)

	CALCULATED			EXPERIMENTAL
	Hartree	Singwi	Singwi*	Cook et al.
T (K)	Screening $R_c = 0.8282$ Å $a = 4.2268$ Å	Screening $R_c = 0.8282$ Å $a = 4.2268$ Å	Screening $R_c = 0.878$ Å $a = 4.225$ Å	(1972)
10	0.00146	0.00210	0.00094	-
20	0.0275	0.0409	0.0220	-
30	0.104	0.156	0.0942	-
40	0.223	0.337	0.215	0.176
50	0.365	0.551	0.361	0.316
60	0.514	0.777	0.518	0.472
70	0.666	1.007	0.678	0.637
80	0.816	1.234	0.836	0.805
90	0.965	1.459	0.993	0.975
100	1.111	1.681	1.148	1.145
120	1.399	2.117	1.451	1.486
140	1.681	2.544	1.748	1.830
160	1.959	2.964	2.040	2.176
180	2.233	3.380	2.329	2.529

TABLE 2.2 - continued

ELECTRICAL RESISTIVITY $\rho(T)$ FOR SODIUM ($\mu\Omega$-cm)

	CALCULATED			EXPERIMENTAL
	Hartree	Singwi	Singwi*	Cook et al.
T	Screening	Screening	Screening	(1972)
(K)	R_c = 0.8282 Å a = 4.2268 Å	R_c = 0.8282 Å a = 4.2268 Å	R_c = 0.878 Å a = 4.225 Å	
200	2.506	3.792	2.615	2.892
260	3.312	5.013	3.462	4.051
300	3.845	5.819	4.021	4.910

*Note: R_c in this case was established by fitting to the resistivity at 100K.

included it is first necessary to establish a more reliable pseudopotential. For this reason the simpler Hartree dielectric function is used with the Ashcroft pseudopotential in the other calculations in this thesis.

CHAPTER III

IMPURITY CALCULATIONS

3.1 Introduction

Employing the isotropic effective phonon distributions of Hayman and Carbotte (1971) it is now possible to extend their techniques to calculate the electrical and thermal resistivity of some alkalis where alkali impurities are included. We consider the case of a dilute alloy by constructing a lattice with one impurity at the origin, and then multiply the final result by the impurity concentration. The calculation ignores the interaction between impurities and the results are valid for the region of up to 1% concentration.

It should be noted that the effect described is of considerably larger magnitude than that discussed by Ekin and Bender (1973) and by Kus and Carbotte (1973). In the latter paper anisotropic frequency distributions are used to investigate systems with very low impurity concentrations relative to the 1% of interest here. They find a washing out of the scattering time anisotropy at their lower concentration.

Although in the present case the calculation is restricted to the alkalis, it bears similarity to the

theoretical treatments of Kagan and Zhernov (1966) and Bhatia and Gupta (1969). However, in the present calculation, a more realistic treatment of the phonons is included and detailed numerical results are provided. Disagreement with the Bhatia-Gupta paper will be discussed in Section 3.4 which deals with the results of the calculation.

3.2 Transport Theory

The theory in this section is based on the work of Ashcroft and Langreth (1967) in liquid metals which was extended by Dynes and Carbotte (1968) and Hayman and Carbotte (1971). In this last paper effective phonon frequency distributions were employed to calculate transport properties in the alkalis.

In extending this work to calculate impurity resistivity, we first assume harmonic phonon theory as discussed in detail in Chapter I. The phonons are empirically determined by inelastic neutron scattering experiments and both the eigenfrequencies and phonon polarization vectors can be calculated using the numerical techniques we have previously considered. Both the eigenfrequencies and polarization vectors will be required when we construct weighted phonon frequency distribution functions.

The interaction of the conduction electrons with the phonons is important in establishing the weighting for transport distribution functions. In the case of the alkalis, we assume that the Fermi surface is spherical and that the conduction electron states are properly described in the single OPW approximation. Using second quantized notation, the electron phonon interaction Hamiltonian is,

$$H_{el\text{-}ph} = \sum_{\underset{\sim}{k},\underset{\sim}{q};\sigma,\lambda} g_{\underset{\sim}{k}+\underset{\sim}{q},\underset{\sim}{k};\lambda}\, C^{\dagger}_{\underset{\sim}{k}+\underset{\sim}{q}\sigma} C_{\underset{\sim}{k}\sigma} (a^{\dagger}_{-\underset{\sim}{q}\lambda} + a_{\underset{\sim}{q}\lambda}) \ , \tag{3.1}$$

where the operators operate on electrons in states $|\underset{\sim}{k}+\underset{\sim}{q}>$ and $|\underset{\sim}{k}>$, and phonons transfer momentum $\underset{\sim}{q}$. The electron phonon coupling constant, which appears in equation (3.1), can be written,

$$g_{\underset{\sim}{k}+\underset{\sim}{q},\underset{\sim}{k};\lambda} = - i[2\omega(\underset{\sim}{q};\lambda)MN]^{-1/2}\underset{\sim}{q}\cdot\underset{\sim}{\varepsilon}(\underset{\sim}{q};\lambda)<\underset{\sim}{k}+\underset{\sim}{q}|w(\underset{\sim}{r})|\underset{\sim}{k}> \quad . \tag{3.2}$$

It contains the pseudopotential and phonon polarization vector. Clearly it is the scattering amplitude for electron phonon scattering.

Hayman and Carbotte (1971) demonstrated the usefulness of using the Ashcroft pseudopotential to calculate transport properties of the alkalis. They employ Hartree screening in the dielectric function and thus ignore many body corrections. The screened electron-ion pseudopotential is written,

$$w(\underset{\sim}{q}) = \frac{-4\pi Ze^2}{\Omega_0 q^2 \varepsilon^*(\underset{\sim}{q})} \cos(qR_c a) \quad , \tag{3.3}$$

where $\varepsilon^*(q)$ is the electron-ion dielectric function. For Hartree screening, $f(\underset{\sim}{q}) = 0$ in equation (2.5) and that equation then reduces to the more conventional form,

$$\varepsilon^*(\underset{\sim}{q}) = 1 + 2v(\underset{\sim}{q})Q(\underset{\sim}{q}) \quad , \tag{3.4}$$

where,

$$v(\underset{\sim}{q}) = \frac{4\pi Ze^2}{q^2} \quad , \tag{3.5}$$

and

$$Q(\underset{\sim}{q}) = \frac{4k_F}{\pi a_0} F(\underset{\sim}{q}) \quad . \tag{3.6}$$

The function $F(\underset{\sim}{q})$ was defined in equation (2.6) and a_0 is the Bohr radius.

Before considering the effect of adding impurities to the calculation of electrical and thermal resistivity we state the results for the ideal case. Following Dynes and Carbotte (1968) electrical resistivity can be written in the form,

$$\rho(T) = C' \sum_{\lambda} \int_{<2k_F} \frac{d^3q q |w(\underset{\sim}{q})|^2 |\underset{\sim}{q}\cdot\underset{\sim}{\varepsilon}(\underset{\sim}{q};\lambda)|^2 \beta}{(e^{\beta\omega(\underset{\sim}{q};\lambda)}-1)(1-e^{-\beta\omega(\underset{\sim}{q};\lambda)})} \quad , \tag{3.7}$$

where,

$$C' = \frac{3\Omega_0}{Me^2 16 v_F^2 k_F^4} \quad , \quad \beta = \frac{\hbar}{k_B T} \quad ,$$

and, $\Omega_0 = \frac{1}{N}$ (the volume per ion). In equation (3.7) the integration over momentum transfer q extends over a sphere of radius $2k_F$ and terms similar to the electron phonon coupling constant can be seen in the numerator.

Following Hayman and Carbotte (1971) an additional integration over all phonon frequencies ω is introduced

and, using the properties of the delta function, equation (3.7) becomes,

$$\rho(T) = C' \int_0^\infty d\omega \sum_\lambda \int_{<2k_F} \frac{d^3q q |w(\underset{\sim}{q})|^2 |\underset{\sim}{q}\cdot\underset{\sim}{\varepsilon}(\underset{\sim}{q};\lambda)|^2 \beta\delta(\omega-\omega(\underset{\sim}{q};\lambda))}{(e^{\beta\omega(\underset{\sim}{q};\lambda)}-1)(1-e^{-\beta\omega(\underset{\sim}{q};\lambda)})} , \tag{3.8}$$

$$\rho(T) = C' \int_0^\infty \frac{\beta d\omega}{(e^{\beta\omega(\underset{\sim}{q};\lambda)}-1)(1-e^{-\beta\omega(\underset{\sim}{q};\lambda)})} \times \sum_\lambda \int_{<2k_F} d^3q \frac{q^2}{2k_F^2} |w(\underset{\sim}{q})|^2 |\underset{\sim}{q}\cdot\underset{\sim}{\varepsilon}(\underset{\sim}{q};\lambda)|^2 \delta(\omega-\omega(\underset{\sim}{q};\lambda)) \tag{3.9}$$

$$\rho(T) = \beta C \int_0^\infty \frac{d\omega\omega\alpha_{tr}^2(\omega)F(\omega)}{(e^{\beta\omega}-1)(1-e^{-\beta\omega})} , \tag{3.10}$$

where,

$$C = \frac{12\pi^3\beta}{e^2 v_F^2 k_F m} .$$

The transport phonon frequency distribution, $\alpha_{tr}^2(\omega)F(\omega)$, is defined by equation (3.11),

$$\alpha_{tr}^2(\omega)F(\omega) = \frac{1}{N}\frac{m}{4Mk_F^3}\sum_\lambda \int_{<2k_F} \frac{q|w(\underset{\sim}{q})|^2 |\underset{\sim}{q}\cdot\underset{\sim}{\varepsilon}(\underset{\sim}{q};\lambda)|^2 \delta(\omega-\omega(\underset{\sim}{q};\lambda))}{2\omega(\underset{\sim}{q};\lambda)} . \tag{3.11}$$

This distribution is more conventional than the $\bar{\alpha}^2(\omega)F(\omega)$ distribution used by Hayman and Carbotte (1971) and has the added advantage of being dimensionless. It has been used

extensively to describe transport properties of the HCP metals, Truant (1972).

Following Baym (1964), the thermal resistivity can be written,

$$W(T) = \frac{1}{L_0 T} C' \sum_{\lambda} \int_{<2k_F} \frac{d^3q |w(\underset{\sim}{q})|^2 \beta |\underset{\sim}{q}\cdot\underset{\sim}{\varepsilon}(\underset{\sim}{q};\lambda)|^2}{(e^{\beta\omega(\underset{\sim}{q};\lambda)}-1)(1-e^{-\beta\omega(\underset{\sim}{q};\lambda)})}$$

$$\times \left[q + \left(\frac{\beta\omega(\underset{\sim}{q};\lambda)}{\pi}\right)^2 \left(\frac{3k_F^2}{q} - \frac{q}{2}\right)\right] \quad , \tag{3.12}$$

where the constant C' is as defined above. Using the familiar $\alpha^2(\omega)F(\omega)$ and $\alpha^2_{tr}(\omega)F(\omega)$ distributions, the thermal resistivity can eventually be expressed in a more useful form,

$$W(T) = \frac{C}{L_0 T} \int_0^{\infty} d\omega\omega \left\{ \frac{(\beta - \frac{\beta^3\pi^2}{2\pi^2})\alpha^2_{tr}(\omega)F(\omega)}{(e^{\beta\omega(\underset{\sim}{q};\lambda)}-1)(1-e^{-\beta\omega(\underset{\sim}{q};\lambda)})} \right.$$

$$\left. + \frac{\frac{3\beta^2\omega^2}{2\pi^2}(1 - \frac{\omega}{V_F k_F})\alpha^2(\omega)F(\omega)}{(e^{\beta\omega(\underset{\sim}{q};\lambda)}-1)(1-e^{-\beta\omega(\underset{\sim}{q};\lambda)})} \right\} \quad . \tag{3.13}$$

The term $-\frac{\omega}{V_F k_F}$ is small and is, therefore, ignored in further calculations. The constant C is defined as above.

3.3 Impurity Calculations

The next step is to generalize the resistivity calculation by considering the interaction of electrons with the lattice vibrations when an impurity ion is included at the origin. The Hamiltonian for the electron-ion interaction is modified by the inclusion of an additional perturbation term,

$$H' = \sum_{\ell} W(\underset{\sim}{r} - \underset{\sim}{R}_{\ell}) + \Delta W(\underset{\sim}{r} - \underset{\sim}{R}_{0}) \quad , \tag{3.14}$$

where,

$$\Delta W = W_i - W_h \quad ,$$

and the subscripts refer to impurity and host pseudopotentials, respectively.

The calculation proceeds by considering the transition probability for electron scattering. This takes place from plane wave states $|\underset{\sim}{k}>$ to $|\underset{\sim}{k}'>$ with momentum transfer q and energy transfer ω such that $\underset{\sim}{q} = \underset{\sim}{k} - \underset{\sim}{k}'$. The Fermi golden rule at finite temperature gives the probability for such a transition,

$$P(\underset{\sim}{q}\omega) = \frac{2\pi}{\hbar^2} \sum_{if} \frac{e^{-\beta\omega_i}}{Z} |<\phi_{f,p-q}|H'|\phi_{i,p}>|^2 \delta(\omega-\omega_{fi}) \quad , \tag{3.15}$$

where $\omega_{fi} = \omega_f - \omega_i$ is the lattice energy change. In equation (3.15) $|\phi_{ip}\rangle$ and $\langle\phi_{f,p-q}|$ are eigenstates of the lattice Hamiltonian with eigenvalues $\hbar\omega_i$ and $\hbar\omega_f$. The system partition function also occurs in equation (3.15) and is defined by equation (3.16) thus,

$$Z = \sum_i e^{-\beta\omega_i} \quad . \tag{3.16}$$

Expanding equation (3.15) we have,

$$\langle\phi_{f,p-q}|H'|\phi_{i,p}\rangle = \sum_\ell \langle\phi_f| \frac{1}{V} \int_{\substack{\text{entire} \\ \text{crystal}}} e^{-i(\underset{\sim}{p}-\underset{\sim}{q})\cdot\underset{\sim}{r}} \times [W(\underset{\sim}{r}-\underset{\sim}{R}_\ell)+\Delta W(\underset{\sim}{r}-\underset{\sim}{R}_0)]e^{i\underset{\sim}{p}\cdot\underset{\sim}{r}} d^3\underset{\sim}{r}|\phi_i\rangle \quad . \tag{3.17}$$

After cancelling factors and recognizing that,

$$V = N\Omega_0 = \text{total volume} \quad , \tag{3.18}$$

the simple change of variables $\underset{\sim}{y} = \underset{\sim}{r} - \underset{\sim}{R}_\ell$ and $d^3\underset{\sim}{y} = d^3\underset{\sim}{r}$ allows us to write,

$$\langle\phi_{f,p-q}|H'|\phi_{i,p}\rangle = \sum_\ell \langle\phi_f| \frac{1}{N\Omega_0} e^{i\underset{\sim}{q}\cdot\underset{\sim}{R}_\ell} \int e^{i\underset{\sim}{q}\cdot\underset{\sim}{y}} W(\underset{\sim}{y}) d^3\underset{\sim}{y}|\phi_i\rangle + \langle\phi_f| \frac{1}{N\Omega_0} e^{i\underset{\sim}{q}\cdot\underset{\sim}{u}_0} \int e^{i\underset{\sim}{q}\cdot\underset{\sim}{y}} \Delta W(\underset{\sim}{y}) d^3\underset{\sim}{y}|\phi_i\rangle \quad . \tag{3.19}$$

We have also made use of the fact that $\underset{\sim}{R}_0 = \underset{\sim}{u}_0$ since $\underset{\sim}{R}_\ell = \underset{\sim}{R}^0_\ell + \underset{\sim}{u}_\ell$ and $\underset{\sim}{R}^0_0 = 0$. The Fourier transform,

$$w(\underset{\sim}{q}) = \frac{1}{\Omega_0} \int_{\substack{\text{entire} \\ \text{crystal}}} e^{i\underset{\sim}{q}\cdot\underset{\sim}{y}} W(\underset{\sim}{y}) d^3\underset{\sim}{y} \quad , \tag{3.20}$$

and similarly for $\Delta w(\underset{\sim}{q})$, allows us to rewrite equation (3.19) as,

$$\langle \phi_{f,p-q} | H' | \phi_{i,p} \rangle = \Sigma \frac{w(\underset{\sim}{q})}{N} \langle \phi_f | e^{i\underset{\sim}{q}\cdot\underset{\sim}{R}_\ell} | \phi_i \rangle + \frac{\Delta w(\underset{\sim}{q})}{N} \langle \phi_f | e^{i\underset{\sim}{q}\cdot\underset{\sim}{u}_0} | \phi_i \rangle \quad . \tag{3.21}$$

Now that the matrix element for electron scattering has been simplified, the entire transition probability can be written,

$$\begin{aligned} P(\underset{\sim}{q}\omega) = \frac{2\pi}{N^2} \sum_{fi} \frac{e^{-\beta\omega_i}}{Z} \delta(\omega-\omega_{fi}) \\ \times \{ |w(\underset{\sim}{q})|^2 \sum_{\ell\ell'} \langle \phi_i | e^{-i\underset{\sim}{q}\cdot\underset{\sim}{R}_\ell} | \phi_f \rangle \langle \phi_f | e^{i\underset{\sim}{q}\cdot\underset{\sim}{R}_{\ell'}} | \phi_i \rangle \\ + w(\underset{\sim}{q}) \Delta w(\underset{\sim}{q}) \sum_{\ell} \langle \phi_i | e^{-i\underset{\sim}{q}\cdot\underset{\sim}{R}_\ell} | \phi_f \rangle \langle \phi_f | e^{i\underset{\sim}{q}\cdot\underset{\sim}{u}_0} | \phi_i \rangle \\ + w(\underset{\sim}{q}) \Delta w(\underset{\sim}{q}) \sum_{\ell} \langle \phi_i | e^{-i\underset{\sim}{q}\cdot\underset{\sim}{u}_0} | \phi_f \rangle \langle \phi_f | e^{i\underset{\sim}{q}\cdot\underset{\sim}{R}_\ell} | \phi_i \rangle \\ + |\Delta w(\underset{\sim}{q})|^2 \langle \phi_i | e^{-i\underset{\sim}{q}\cdot\underset{\sim}{u}_0} | \phi_f \rangle \langle \phi_f | e^{i\underset{\sim}{q}\cdot\underset{\sim}{u}_0} | \phi_i \rangle \} \quad . \end{aligned} \tag{3.22}$$

The well known Van Hove technique is now employed to convert from the Schrödinger to the Heisenberg representation. In general, we can write,

$$\langle\phi_i|e^{iH_0t}e^{-i\underset{\sim}{q}\cdot\underset{\sim}{R}_\ell}e^{-iH_0t}|\phi_f\rangle \equiv \langle\phi_i|e^{-i\underset{\sim}{q}\cdot\underset{\sim}{R}_\ell(t)}|\phi_f\rangle \quad ,$$

$$\langle\phi_i|e^{-i\underset{\sim}{q}\cdot\underset{\sim}{R}_\ell(t)}|\phi_f\rangle = e^{i\omega_i t}e^{-i\omega_f t}\langle\phi_i|e^{-i\underset{\sim}{q}\cdot\underset{\sim}{R}_\ell}|\phi_f\rangle \quad ,$$

$$\langle\phi_i|e^{-i\underset{\sim}{q}\cdot\underset{\sim}{R}_\ell}|\phi_f\rangle = e^{i\omega_{fi}t}\langle\phi_i|e^{-i\underset{\sim}{q}\cdot\underset{\sim}{R}_\ell(t)}|\phi_f\rangle \quad . \qquad (3.23)$$

Employing equations (3.23) we can now write the first term of equation (3.22),

$$P^{(1)}(\underset{\sim}{q}\omega) = \frac{2\pi}{N^2}\sum_{fi}\frac{e^{-\beta\omega_i}}{Z}\delta(\omega-\omega_{fi})e^{i\omega_{fi}t}$$

$$\times |w(\underset{\sim}{q})|^2 \sum_{\ell\ell'}\langle\phi_i|e^{-i\underset{\sim}{q}\cdot\underset{\sim}{R}_\ell(t)}|\phi_f\rangle$$

$$\times \langle\phi_f|e^{i\underset{\sim}{q}\cdot\underset{\sim}{R}_{\ell'}}|\phi_i\rangle \quad . \qquad (3.24)$$

We now introduce the convenient notation,

$$S^{(1)}(\underset{\sim}{q}\omega) = \sum_{fi}\frac{e^{-\beta\omega_i}}{Z}\delta(\omega-\omega_{fi})e^{i\omega_{fi}t}$$

$$\times \sum_{\ell\ell'}\langle\phi_i|e^{-i\underset{\sim}{q}\cdot\underset{\sim}{R}_\ell(t)}|\phi_f\rangle\langle\phi_f|e^{i\underset{\sim}{q}\cdot\underset{\sim}{R}_{\ell'}}|\phi_i\rangle \quad , \qquad (3.25)$$

which allows us to construct the Fourier transform pair,

$$S^{(1)}(\underset{\sim}{q}t) = \frac{1}{2\pi}\int_{-\infty}^{\infty} d\omega e^{-i\omega t} S^{(1)}(\underset{\sim}{q}\omega) \quad ,$$

$$S^{(1)}(\underset{\sim}{q}\omega) = \int_{-\infty}^{\infty} dt e^{i\omega t} S^{(1)}(\underset{\sim}{q}t) \quad . \tag{3.26}$$

Using this new convenient notation, the entire transition probability expression becomes,

$$P(\underset{\sim}{q}\omega) = \frac{2\pi}{N^2}\{|w(\underset{\sim}{q})|^2 S^{(1)}(\underset{\sim}{q}\omega) + w(\underset{\sim}{q})\Delta w(\underset{\sim}{q}) S^{(2)}(\underset{\sim}{q}\omega)$$

$$+ w(\underset{\sim}{q})\Delta w(\underset{\sim}{q}) S^{(3)}(\underset{\sim}{q}\omega) + |\Delta w(\underset{\sim}{q})|^2 S^{(4)}(\underset{\sim}{q}\omega)\} \quad . \tag{3.27}$$

We now direct our attention to factors of the form defined in equation (3.25). The Fourier transform of this equation is written,

$$S^{(1)}(\underset{\sim}{q}t) = \frac{1}{2\pi}\int_{-\infty}^{\infty} d\omega e^{-i\omega t} \sum_{fi} \frac{e^{-\beta\omega_i}}{Z} \delta(\omega-\omega_{fi}) e^{i\omega_{fi}t}$$

$$\times \sum_{\ell\ell'} \langle\phi_i| e^{-i\underset{\sim}{q}\cdot\underset{\sim}{R}_\ell(t)} |\phi_f\rangle\langle\phi_f| e^{i\underset{\sim}{q}\cdot\underset{\sim}{R}_{\ell'}} |\phi_i\rangle \quad . \tag{3.28}$$

Noting that,

$$\int d\omega e^{-i(\omega-\omega_{fi})t} \delta(\omega-\omega_{fi}) = 1 \quad ,$$

and $$\tag{3.29}$$

$$\sum_f |\phi_f\rangle\langle\phi_f| = 1 \quad ,$$

equation (3.28) can be rewritten as,

$$S^{(1)}(\underset{\sim}{q}t) = \frac{1}{2\pi} \sum_i \frac{e^{-\beta\omega_i}}{Z} \sum_{\ell\ell'} \langle\phi_i| e^{-i\underset{\sim}{q}\cdot\underset{\sim}{R}_\ell(t)} e^{i\underset{\sim}{q}\cdot\underset{\sim}{R}_{\ell'}} |\phi_i\rangle \quad . \tag{3.30}$$

In general, a thermal average is expressed in the form,

$$\langle A\rangle_T = \sum_i \frac{e^{-\beta\omega_i}}{Z} \langle\phi_i|A|\phi_i\rangle \quad . \tag{3.31}$$

Clearly we can now write equation (3.30) as a thermal average,

$$S^{(1)}(\underset{\sim}{q}t) = \frac{1}{2\pi} \sum_{\ell\ell'} \langle e^{-i\underset{\sim}{q}\cdot\underset{\sim}{R}_\ell(t)} e^{i\underset{\sim}{q}\cdot\underset{\sim}{R}_{\ell'}} \rangle_T \quad . \tag{3.32}$$

The other Fourier transform terms then follow analogously,

$$\begin{aligned} S^{(2)}(\underset{\sim}{q}t) &= \frac{1}{2\pi} \sum_\ell \langle e^{-i\underset{\sim}{q}\cdot\underset{\sim}{R}_\ell(t)} e^{i\underset{\sim}{q}\cdot\underset{\sim}{u}_0} \rangle_T \quad , \\ S^{(3)}(\underset{\sim}{q}t) &= \frac{1}{2\pi} \sum_\ell \langle e^{-i\underset{\sim}{q}\cdot\underset{\sim}{u}_0(t)} e^{i\underset{\sim}{q}\cdot\underset{\sim}{R}_\ell} \rangle_T \quad , \\ S^{(4)}(\underset{\sim}{q}t) &= \frac{1}{2\pi} \langle e^{-i\underset{\sim}{q}\cdot\underset{\sim}{u}_0(t)} e^{i\underset{\sim}{q}\cdot\underset{\sim}{u}_0} \rangle_T \quad . \end{aligned} \tag{3.33}$$

If we consider only the $S^{(1)}(\underset{\sim}{q}t)$ term, expand the exponentials to lowest order, and retain only the dynamic time dependent parts, we have,

$$e^{-i\underset{\sim}{q}\cdot\underset{\sim}{R}_\ell(t)} \approx e^{-i\underset{\sim}{q}\cdot\underset{\sim}{R}^0_\ell}(1 - i\underset{\sim}{q}\cdot\underset{\sim}{u}_\ell(t)) \quad . \tag{3.34}$$

Similar expansions can be made for the other expressions in equation (3.33). Applying the result of equation (3.34) to $S^{(1)}(\underset{\sim}{q}t)$ we have the result,

$$S^{(1)}(\underset{\sim}{q}t) = \frac{1}{2\pi}\sum_{\ell\ell'} e^{-i\underset{\sim}{q}\cdot\underset{\sim}{R}^0_\ell} e^{i\underset{\sim}{q}\cdot\underset{\sim}{R}^0_{\ell'}}$$

$$\times \langle(1 - i\underset{\sim}{q}\cdot\underset{\sim}{u}_\ell(t))(1 + i\underset{\sim}{q}\cdot\underset{\sim}{u}_{\ell'})\rangle_T \quad . \tag{3.35}$$

If we consider the product for which we take the thermal average times the remainder of the expression, it can be seen that the first term gives the Bragg peak and the second and third terms are zero since, $\langle\underset{\sim}{u}_\ell(t)\rangle_T = 0$. We are left with,

$$S^{(1)}(\underset{\sim}{q}t) = \frac{1}{2\pi}\sum_{\ell\ell'} e^{-i\underset{\sim}{q}\cdot\underset{\sim}{R}^0_\ell} e^{i\underset{\sim}{q}\cdot\underset{\sim}{R}^0_{\ell'}} \langle\underset{\sim}{q}\cdot\underset{\sim}{u}_\ell(t)\underset{\sim}{q}\cdot\underset{\sim}{u}_{\ell'}\rangle_T \quad . \tag{3.36}$$

Following Dynes and Carbotte (1968) we can express the displacements, $\underset{\sim}{u}_\ell(t)$, in terms of phonon creation and annihilation operators,

$$\sum_\ell e^{-i\underset{\sim}{q}\cdot\underset{\sim}{\ell}}(-i)\underset{\sim}{q}\cdot\underset{\sim}{u}_\ell(t) = \sum_\lambda \left\{\frac{N}{2M\omega(\underset{\sim}{q};\omega)}\right\}^{1/2}$$

$$\times (-i)\underset{\sim}{q}\cdot\underset{\sim}{\varepsilon}(\underset{\sim}{q};\lambda)[a^\dagger_{-\underset{\sim}{q}\lambda}(t) + a_{\underset{\sim}{q}\lambda}(t)] \quad , \tag{3.37}$$

where q is to be read as reduced to the FBZ when labelling the phonon operators. For an harmonic system the thermal averaged product of phonon operators can be expressed as,

$$\langle a^{\dagger}_{\underset{\sim}{k}\lambda} a_{\underset{\sim}{k}'\lambda'} \rangle_T = n[\omega(\underset{\sim}{k};\lambda)]\delta_{kk'}\delta_{\lambda\lambda'}$$

$$= \frac{\delta_{kk'}\delta_{\lambda\lambda'}}{(e^{\beta\omega(\underset{\sim}{k};\lambda)}-1)} \quad , \tag{3.38}$$

which is the Bose Einstein population. We now combine equations (3.36), (3.37) and (3.38) and Fourier transform to get,

$$S^{(1)}(\underset{\sim}{q}\omega) = \sum_{\lambda} \frac{|\underset{\sim}{q}\cdot\underset{\sim}{\varepsilon}(\underset{\sim}{q};\lambda)|^2}{2M\omega(\underset{\sim}{q};\lambda)} N\{(n[\omega(\underset{\sim}{q};\lambda)]+1)\delta(\omega-\omega(\underset{\sim}{q};\lambda))$$

$$+ n[\omega(\underset{\sim}{q};\lambda)]\delta(\omega+\omega(\underset{\sim}{q};\lambda))\} \quad . \tag{3.39}$$

The time dependence of the phonon operators, (explicit in equation (3.37)), is contained in exponential factors which disappear when we Fourier transform.

We now examine the other three factors which can be treated in an exactly analogous manner. It can readily be shown that,

$$S^{(2)}(\underset{\sim}{q}\omega) = S^{(3)}(\underset{\sim}{q}\omega) = \sum_{\lambda} \frac{|\underset{\sim}{q}\cdot\underset{\sim}{\varepsilon}(\underset{\sim}{q};\lambda)|^2}{2M\omega(\underset{\sim}{q};\lambda)}$$

$$\times \{(n[\omega(\underset{\sim}{q};\lambda)]+1)\delta(\omega-\omega(\underset{\sim}{q};\lambda)) + n[\omega(\underset{\sim}{q};\lambda)]\delta(\omega+\omega(\underset{\sim}{q};\lambda))\} \quad , \tag{3.40}$$

and, $$S^{(4)}(\underset{\sim}{q}\omega) = \sum_{k,\lambda} \frac{|\underset{\sim}{q}\cdot\underset{\sim}{\varepsilon}(\underset{\sim}{k};\lambda)|^2}{2MN\omega(\underset{\sim}{k};\lambda)}$$

$$\times \{(n[\omega(\underset{\sim}{k};\lambda)]+1)\delta(\omega-\omega(\underset{\sim}{k};\lambda)) + n[\omega(\underset{\sim}{k};\lambda)]\delta(\omega+\omega(\underset{\sim}{k};\lambda))\} . \tag{3.41}$$

The significant difference between these factors is the contribution of factors of N from the sums over ℓ and ℓ'. Since the last factor, $S^{(4)}(\underset{\sim}{q}\omega)$, does not involve a sum over ℓ or ℓ' we are left with a single Brillouin Zone sum over $\underset{\sim}{k}$.

At this point we can see immediately how to apply the formulation thus far developed. A very general expression for the electrical resistivity includes the transition probability explicitly,

$$\rho(T) = \frac{C\hbar\beta N}{M2\pi} \int_{<2k_F} d^3q\, q \sum_{\lambda} \int_{-\infty}^{\infty} \frac{d\omega\omega P(\underset{\sim}{q}\omega)}{(e^{\beta\omega(\underset{\sim}{q};\lambda)}-1)} , \tag{3.42}$$

where C is left arbitrary for the present. In the simple pure case we employ only the first term on the right hand side of equation (3.27) to get,

$$\rho(T) = \frac{C\hbar\beta}{MN} \int_{<2k_F} d^3q\, q |w(\underset{\sim}{q})|^2 \sum_{\lambda} \int_{-\infty}^{\infty} \frac{d\omega\omega S^{(1)}(\underset{\sim}{q}\omega)}{(e^{\beta\omega(\underset{\sim}{q};\lambda)}-1)} . \tag{3.43}$$

It can be seen readily that this equation (which was used by Dynes and Carbotte (1968)) immediately leads to equation (3.7).

In constructing equation (3.10) we have introduced an additional integration over the delta function which allows

us to isolate a phonon frequency distribution, (equations (1.24), (1.26) and (3.11)), from the temperature dependence of the resistivity expression. When we deal with the new contributions from $P(\underset{\sim}{q};\omega)$ it is convenient to introduce two auxiliary phonon frequency distribution functions, $\alpha'^2(\omega)F(\omega)$ and $\alpha'^2_{tr}(\omega)F(\omega)$. These distributions arise through the substitution of $w(\underset{\sim}{q})\Delta w(\underset{\sim}{q})S^{(2,3)}(\underset{\sim}{q};\omega)$ for the usual $|w(\underset{\sim}{q})|^2 S^{(1)}(\underset{\sim}{q};\omega)$. We write down the auxiliary distribution functions so that we can use them later in calculations of impurity modified resistivities.

$$\alpha'^2_{tr}(\omega)F(\omega) = \frac{1m}{N^2 4Mk_F^3} \sum_{\lambda} \int \frac{d^3q}{(2\pi)^3} q \frac{|w(\underset{\sim}{q})\Delta w(\underset{\sim}{q})|}{2\omega(\underset{\sim}{q};\lambda)} \times |\underset{\sim}{q}\cdot\underset{\sim}{\varepsilon}(\underset{\sim}{q};\lambda)|^2 \delta(\omega-\omega(\underset{\sim}{q};\lambda)) \quad . \tag{3.44}$$

The second distribution function occurs only in the calculation of thermal resistivity,

$$\alpha'^2(\omega)F(\omega) = \frac{1m}{N^2 4Mk_F} \sum_{\lambda} \int_{<2k_F} \frac{d^3q}{(2\pi)^3} \frac{|w(\underset{\sim}{q})\Delta w(\underset{\sim}{q})|}{\underset{\sim}{q}\omega(\underset{\sim}{q};\lambda)} \times |\underset{\sim}{q}\cdot\underset{\sim}{\varepsilon}(\underset{\sim}{q};\lambda)|^2 \delta(\omega-\omega(\underset{\sim}{q};\lambda)) \quad . \tag{3.45}$$

We now consider the contribution of the final structure factor arising from $P(q;\omega)$, namely $S^{(4)}(\underset{\sim}{q};\omega)$. We substitute it into equation (3.42),

$$\rho^{(4)}(T) = \frac{C\hbar\beta}{MN^2}\int d^3\underset{\sim}{q}q\,|\Delta w(\underset{\sim}{q})|^2 \sum_{k,\lambda}\int \frac{d\omega\omega S^4(\underset{\sim}{q};\omega)}{(e^{\beta\omega(\underset{\sim}{q};\lambda)}-1)} \quad . \tag{3.46}$$

After performing the angular integration and appropriately collecting terms we are left with,

$$\rho^{(4)}(T) = \frac{C\hbar\beta x}{MN}\frac{4\pi}{3}\int_{<2k_F} dq q^5 |\Delta w(q)|^2 \times \int d\omega \frac{F(\omega)}{(e^{\beta\omega(\underset{\sim}{q};\lambda)}-1)(1-e^{-\beta\omega(\underset{\sim}{q};\lambda)})} \quad , \tag{3.47}$$

where the right hand side of the equation has been scaled so that ρ is in terms of impurity concentration x.

We can now quote the results, for both the electrical and thermal cases, of the addition of impurities to the resistivity. First we state the electrical case with the equation scaled in terms of impurity concentration,

$$\rho_{IMP}(T) = C\rho\beta\int_0^\infty \frac{d\omega\omega}{(e^{\beta\omega(\underset{\sim}{q};\lambda)}-1)(1-e^{-\beta\omega(\underset{\sim}{q};\tau)})}\alpha^2_{tr}(\omega)F(\omega) + C\rho\beta x\int_0^\infty \frac{d\omega\omega}{(e^{\beta\omega(\underset{\sim}{q};\lambda)}-1)(1-e^{-\beta\omega(\underset{\sim}{q};\lambda)})}\alpha'^2_{tr}(\omega)F(\omega) + \frac{C\rho\beta x}{N}\frac{4\pi}{3}\int_0^\infty dq q^5|\Delta w(q)|^2 \times \int_{<2k_F} d\omega \frac{F(\omega)}{(e^{\beta\omega(\underset{\sim}{q};\lambda)}-1)(1-e^{-\beta\omega(\underset{\sim}{q};\lambda)})} \quad , \tag{3.48}$$

where $C\rho = \dfrac{12\pi^3\beta}{e^2v_F^2k_Fm}$.

In an exactly analogous manner we can write the result for the thermal case,

$$W_{IMP}(T) = \frac{C_W}{L_0 T}\{\int_0^\infty \frac{d\omega}{(e^{\beta\omega(\tilde{q};\lambda)}-1)(1-e^{-\beta\omega(\tilde{q};\lambda)})}$$

$$\times [(\beta - \frac{\beta^3\omega^2}{2\pi^2})\alpha^2_{tr}(\omega)F(\omega) + x(\beta - \frac{\beta^3\omega^2}{2\pi^2})\alpha'^2_{tr}(\omega)F(\omega)$$

$$+ \frac{3\beta^3\omega^2}{2\pi^2}\alpha^2(\omega)F(\omega) + \frac{x3\beta^3\omega^2}{2\pi^2}\alpha'^2(\omega)F(\omega)]\}$$

$$+ \frac{C_W x}{L_0 TN}\frac{4\pi}{3}\{\int_0^\infty dq q^5 |\Delta w(q)|^2$$

$$\times \int_{<2k_F} d\omega \frac{F(\omega)}{(e^{\beta\omega(\tilde{q};\lambda)}-1)(1-e^{-\beta\omega(\tilde{q};\lambda)})}(\beta - \frac{\beta^3\omega^2}{2\pi^2})$$

$$+ \int_0^\infty dq q^3 |\Delta w(q)|^2 \int_{<2k_F} d\omega$$

$$\times \frac{F(\omega)}{(e^{\beta\omega(\tilde{q};\lambda)}-1)(1-e^{-\beta\omega(\tilde{q};\lambda)})}(\frac{3\beta^3\omega^2}{2\pi^2}) \quad , \tag{3.49}$$

where, $C_W = \frac{12\pi^3\beta}{e^2 v_F^2 k_F m}$.

At this point it is worth noting the expression for the residual electrical resistivity. It is similar to the final term in equation (3.48), and can be expressed as,

$$\rho_0 = \frac{3\pi m\Omega_0}{8he^2 E_F k_F^4}\int_0^{2k_F} dq q^3 |\Delta w(q)|^2 \quad . \tag{3.50}$$

In general the total resistivity is related to the residual resistivity by,

$$\rho_{TOTAL}(T) = \rho(T) + \rho_0 \quad , \tag{3.51}$$

where $\rho(T)$ is the resistivity of the pure metal and corresponds to $\rho(T)$ of equations (3.10) and (3.43). Impurity concentration is assumed small and ρ_0 is independent of temperature. Equation (3.51) is essentially a statement of 'Matthiessen's Rule', MR. According to the equation the addition of impurities adds a constant component to the total resistivity leaving the temperature dependent component unchanged.

For some time, however, it has been known that deviations to this rule exist. A more appropriate equation is then,

$$\rho_{IMP}(x,T) = \rho(T) + \rho_0(x) + \Delta(x,T) \quad , \tag{3.52}$$

where Δ is the 'Deviation from Matthiessen's Rule', and the equation now contains an explicit impurity concentration dependence. It should be noted that the second term on the right of equation (3.48) contributes a deviation from MR as does the phonon frequency contribution of the third term.

3.4 Results

Calculations have been made of electrical and thermal impurity resistivity for several alkali - alkali systems. The results are displayed in graphical form and we will discuss them in groups of impurity-host combination.

Several assumptions should be emphasized at this point. First pseudopotentials have been calculated using the Hartree dielectric function, so clearly many body effects are ignored. Also mass change effects are not considered. Because of this we have ignored systems where the mass difference is very large, although it should be emphasized that in all cases the difference is generally at least a factor of two.

Another important limitation which has been mentioned before, but bears repeating, is that the calculation ignores the interaction between impurities in the dilute alloy systems.

From the calculations several important characteristics of impurity systems have become apparent. First and most important, is the sensitivity of impurity dependent properties on the difference between the host and impurity pseudopotential. If the difference is small, the result of adding impurities is negligible. The resulting impurity electrical and thermal resistivities are essentially the same as those calculated for the pure case.

A second important characteristic is a dependence of impurity properties on the relative magnitudes of host and impurity pseudopotentials. If the impurity pseudopotential is greater than that of the host then the contributions of the $w(\underset{\sim}{q})\Delta w(\underset{\sim}{q})$ terms will be negative. In this case the auxiliary distributions will also be negative and the contribution of impurities to the electrical and thermal resistivity will be relatively smaller than in the case of positive contributions from the $w(\underset{\sim}{q})\Delta w(\underset{\sim}{q})$ terms.

We now consider in detail three systems which display the properties I have described. The first system is that of potassium with a lithium impurity. The pseudopotential difference in this case, Figure (3.1), is insignificant so the effect of adding impurities is negligible. In the electrical case, Figure (3.2), and the thermal case, Figure (3.3), the contributions from the $w(\underset{\sim}{q})\Delta w(\underset{\sim}{q})$ and $|\Delta w(\underset{\sim}{q})|^2$ terms are roughly equal and small, relative to the pure resistivities. The residual resistivity in this case is also small since it is dependent on the $|\Delta w(\underset{\sim}{q})|^2$ factor.

The next system under consideration is potassium with a sodium impurity. In this system the pseudopotential difference becomes significant at $2k_F$ as can be seen in Figure (3.4). Also it should be noted that $w(\underset{\sim}{q})_{HOST}$ is greater than $w(\underset{\sim}{q})_{IMPURITY}$ so the contribution from $w(\underset{\sim}{q})\Delta w(\underset{\sim}{q})$ terms will be positive. The resulting distribution

Fig. 3.1 Hartree screened Ashcroft pseudopotentials for the system of potassium with a lithium impurity

Potassium ———

$R_c = 1.0353 \quad a = 5.2275$

Lithium . . .

$R_c = 1.000353 \quad a = 5.2275$.

Fig. 3.1

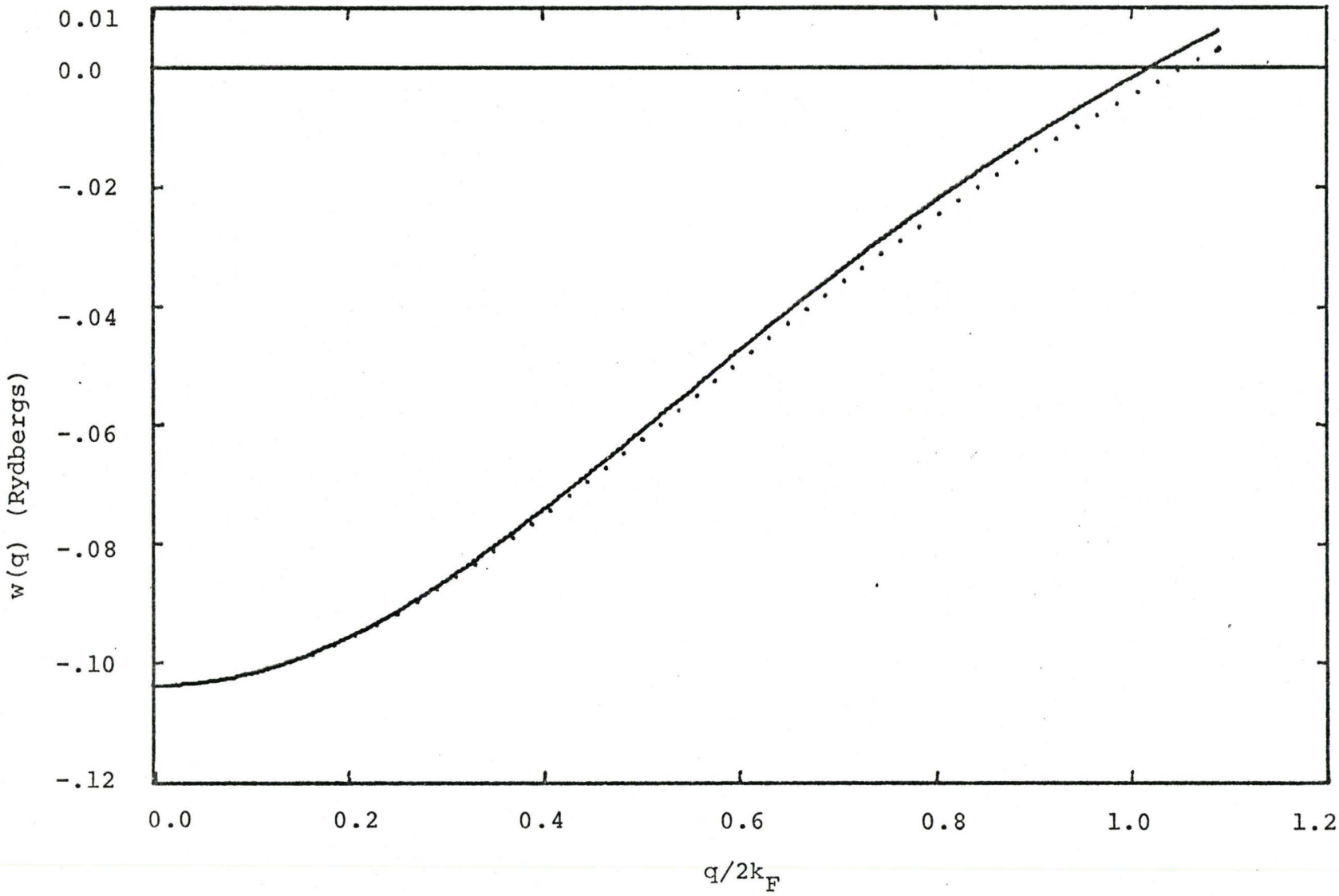

Fig. 3.2 Impurity term contributions to the electrical resistivity for potassium with a lithium impurity

$\rho_{w\Delta w}$ ———

$\rho_{\Delta w^2}$ . . .

$\rho_{w\Delta w} + \rho_{\Delta w^2}$ - - -

Fig. 3.2

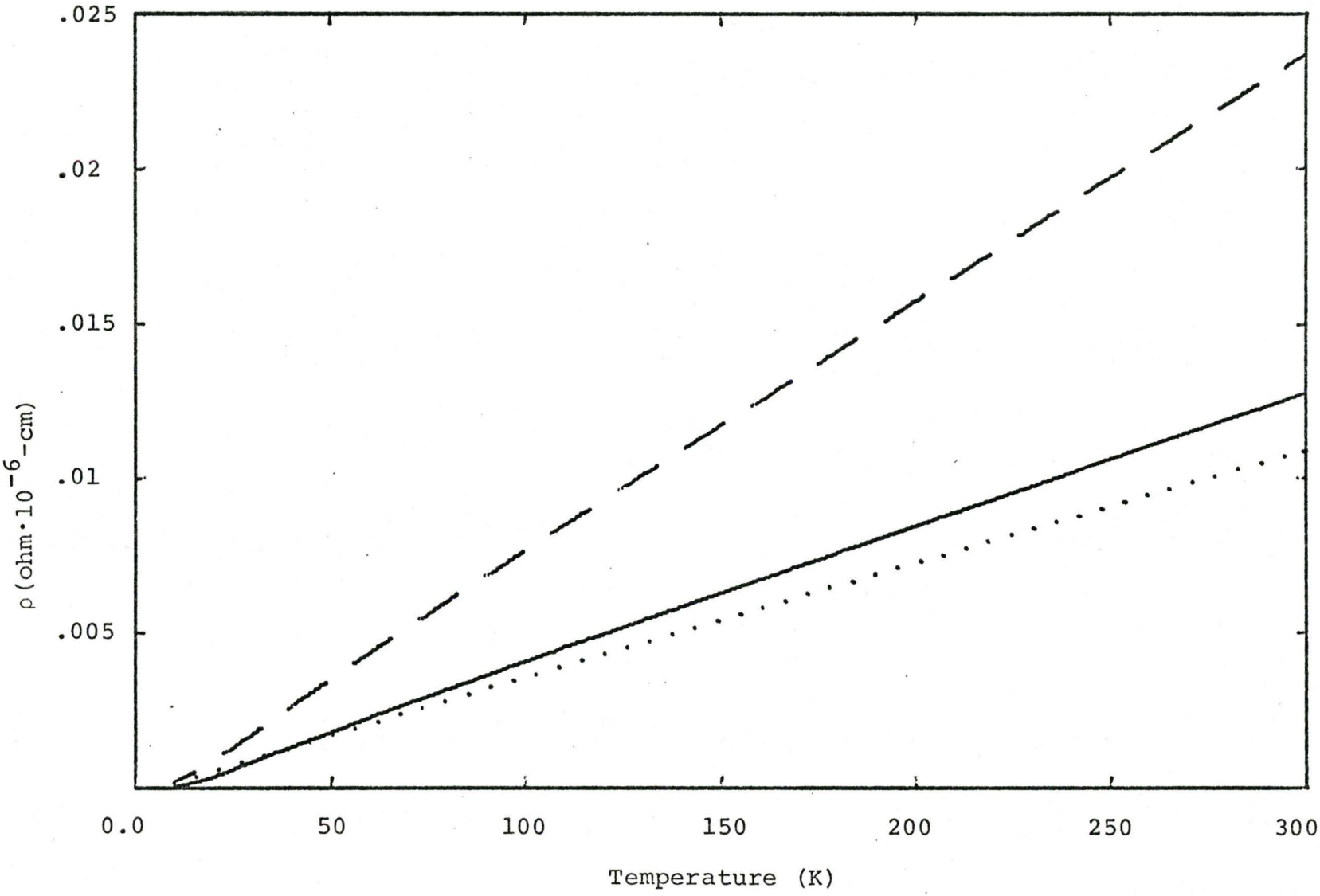
.025
.02
.015
.01
.005
ρ (ohm·10⁻⁶-cm)
0.0
50
100
150
200
250
300
Temperature (K)

Fig. 3.3 Impurity term contributions to the thermal resistivity for potassium with a lithium impurity

$W_{w\Delta w}$ ———

$W_{\Delta w^2}$ . . .

$W_{w\Delta w} + W_{\Delta w^2}$ - - -

Fig. 3.3

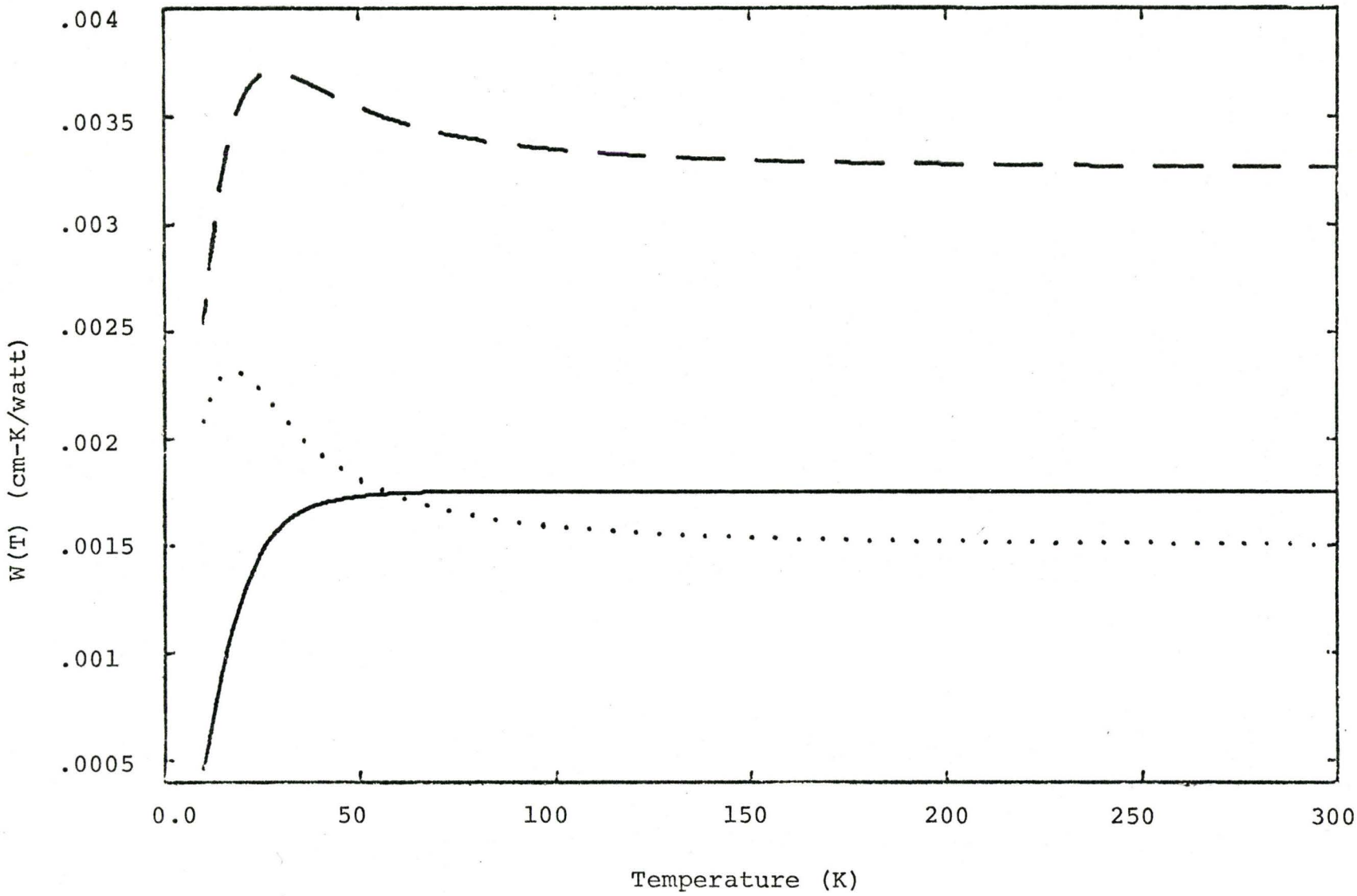
.004
.0035
.003
.0025
.002
.0015
.001
.0005
W(T) (cm-K/watt)
0.0
50
100
150
200
250
300
Temperature (K)

Fig. 3.4 Hartree screened Ashcroft pseudopotentials for the system of potassium with a sodium impurity

Potassium ———

R_c = 1.0353 a = 5.2275

Sodium . . .

R_c = 0.8282 a = 5.2275 .

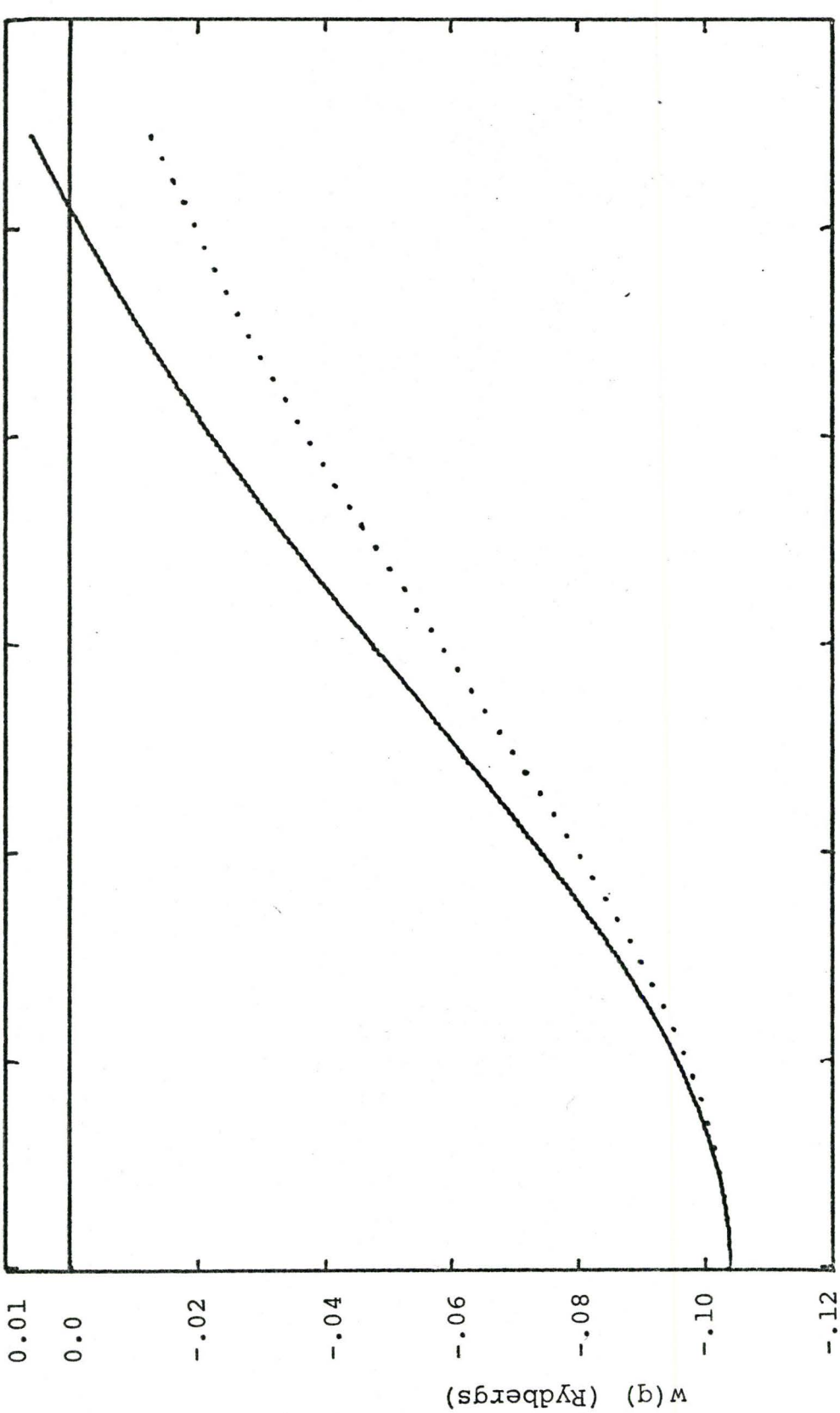

Fig. 3.4

functions and auxiliary distribution functions are plotted in Figures (3.5) and (3.6). As one would expect, the auxiliary distributions are positive and bear great similarity to the principle distributions $\alpha^2_{tr}(\omega)F(\omega)$ and $\alpha^2(\omega)F(\omega)$.

In Figure (3.7) the $w(\underset{\sim}{q})\Delta w(\underset{\sim}{q})$ and $|\Delta w(\underset{\sim}{q})|^2$ contributions to the electrical resistivity are plotted and it can be seen in Figure (3.8) that these terms make a contribution to the total resistivity which is roughly equal to that of the residual resistivity for higher temperatures. The importance of Figure (3.8) is that it shows a significant deviation from Matthiessen's Rule at temperatures as low as 40 degrees.

In Figure (3.9) the contributions to the thermal resistivity of the $w(\underset{\sim}{q})\Delta w(\underset{\sim}{q})$ term are positive as we would expect. As in the electrical case, the $|\Delta w(\underset{\sim}{q})|^2$ term is significant relative to the pure thermal resistivity. This can be seen in Figure (3.10).

We now turn our attention to the reverse situation where the host is sodium and the impurity potassium. In Figure (3.11) it is clear that the host-impurity pseudopotential difference is significant. The interesting fact in this case is that the impurity pseudopotential is greater than that of the host. This leads to negative contributions from $w(\underset{\sim}{q})\Delta w(\underset{\sim}{q})$ terms with interesting consequences as we shall see.

Fig. 3.5 Frequency distributions for potassium with a sodium impurity.

Hartree screened Ashcroft pseudopotential

$R_c = 1.0353$ $a = 5.2275$

$F(\nu)$ ———

$\alpha^2_{tr}(\nu)F(\nu)$ . . .

$\alpha^2(\nu)F(\nu)$ - - -

Fig. 3.5

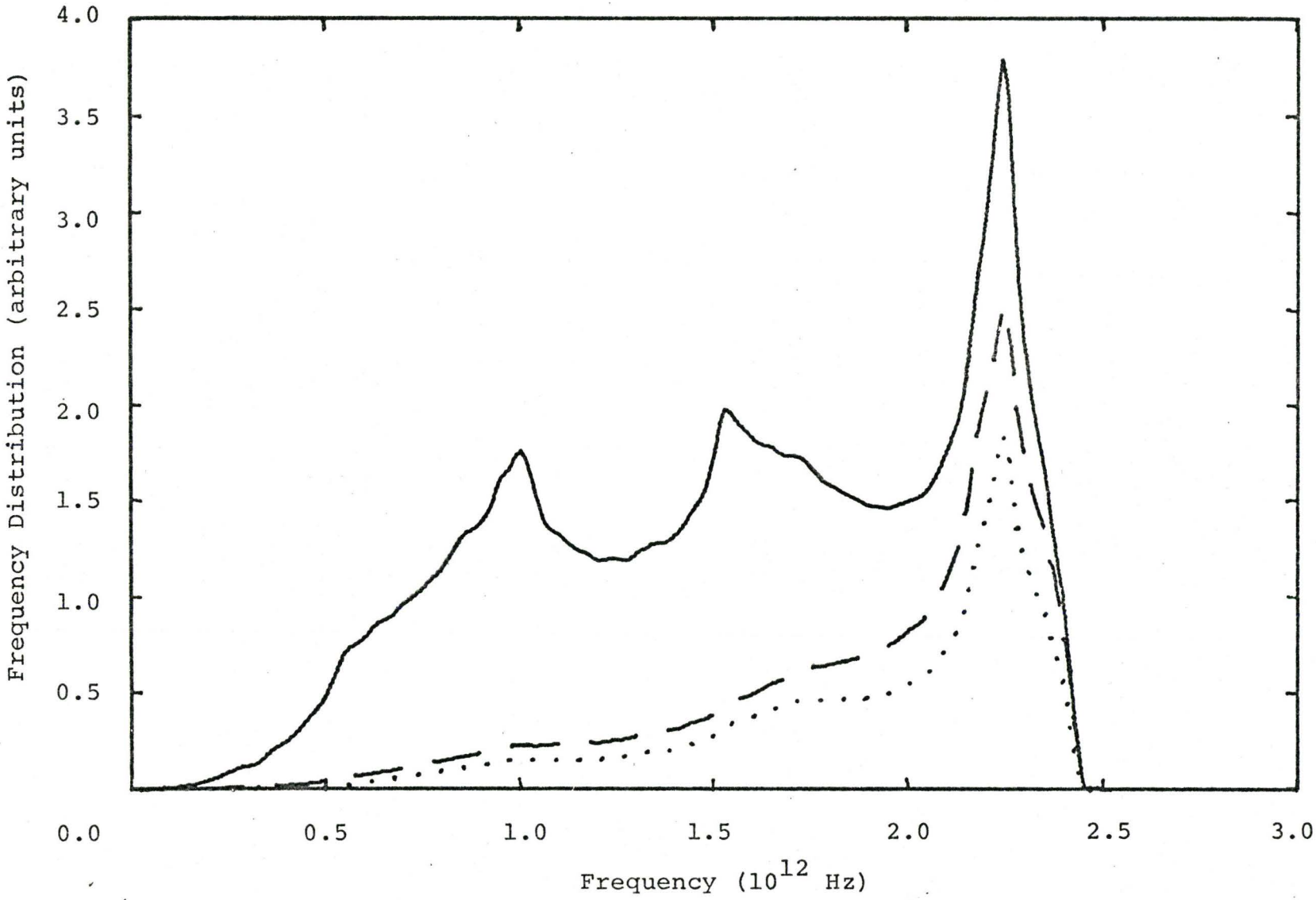
Frequency Distribution (arbitrary units)
4.0
3.5
3.0
2.5
2.0
1.5
1.0
0.5
0.0
0.5
1.0
1.5
2.0
2.5
3.0
Frequency (10^{12} Hz)

Fig. 3.6 Auxiliary frequency distributions for potassium with a sodium impurity
Hartree screened Ashcroft pseudopotential

$F(\nu)$ ———

$\alpha'^2_{tr}(\nu)F(\nu)$ . . .

$\alpha'^2(\nu)F(\nu)$ - - -

Note: $\alpha'^2_{tr}(\nu)F(\nu)$ and $\alpha'^2(\nu)F(\nu)$ have been scaled up by a factor of 10.

Fig. 3.6

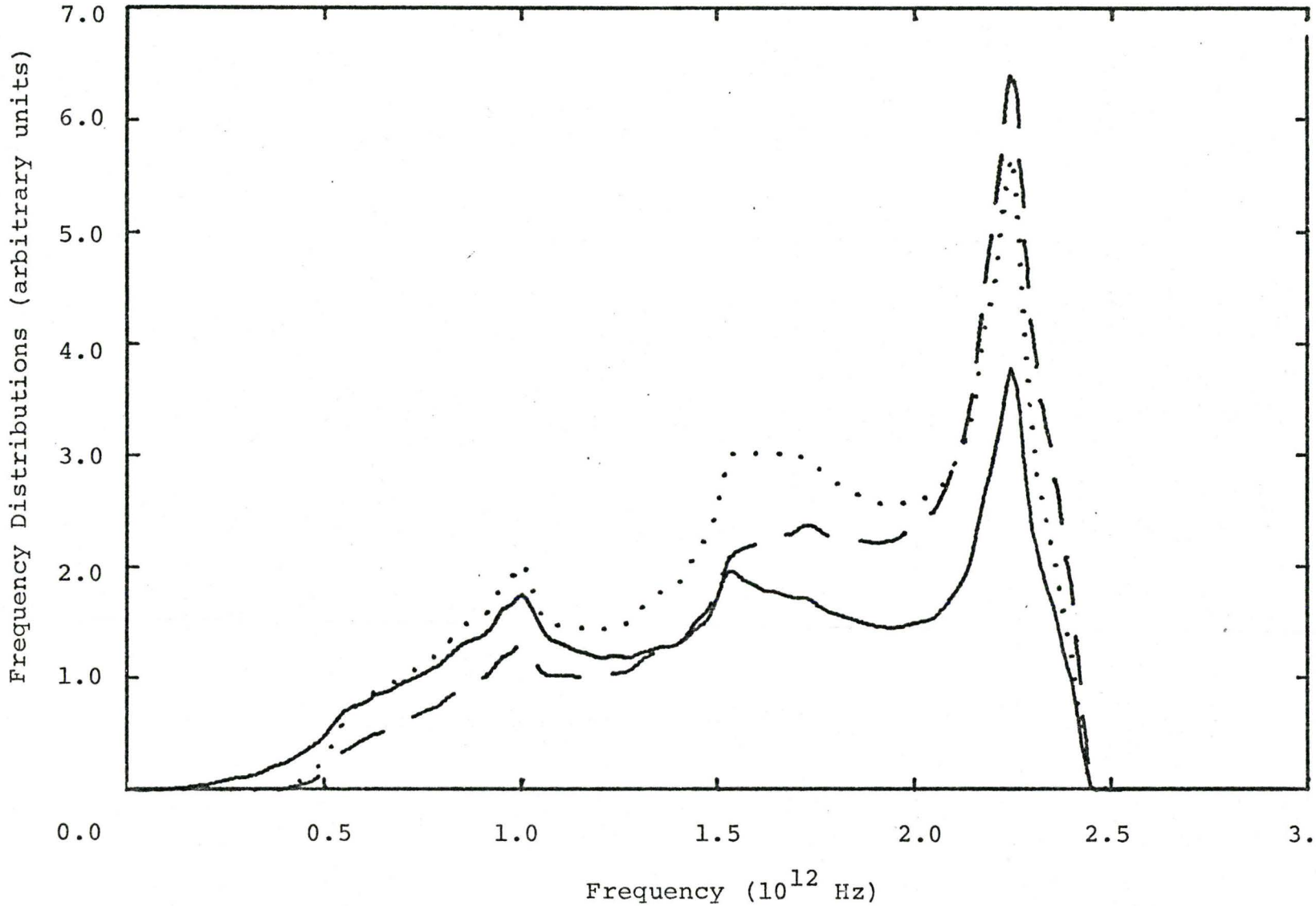
Frequency Distributions (arbitrary units)
7.0
6.0
5.0
4.0
3.0
2.0
1.0
0.0
0.5
1.0
1.5
2.0
2.5
3.0
Frequency (10^{12} Hz)

Fig. 3.7 Impurity term contributions to the electrical resistivity for potassium with a sodium impurity

$\rho_{w\Delta w}$ ———

$\rho_{\Delta w^2}$ . . .

$\rho_{w\Delta w} + \rho_{\Delta w^2}$ - - -

Fig. 3.7

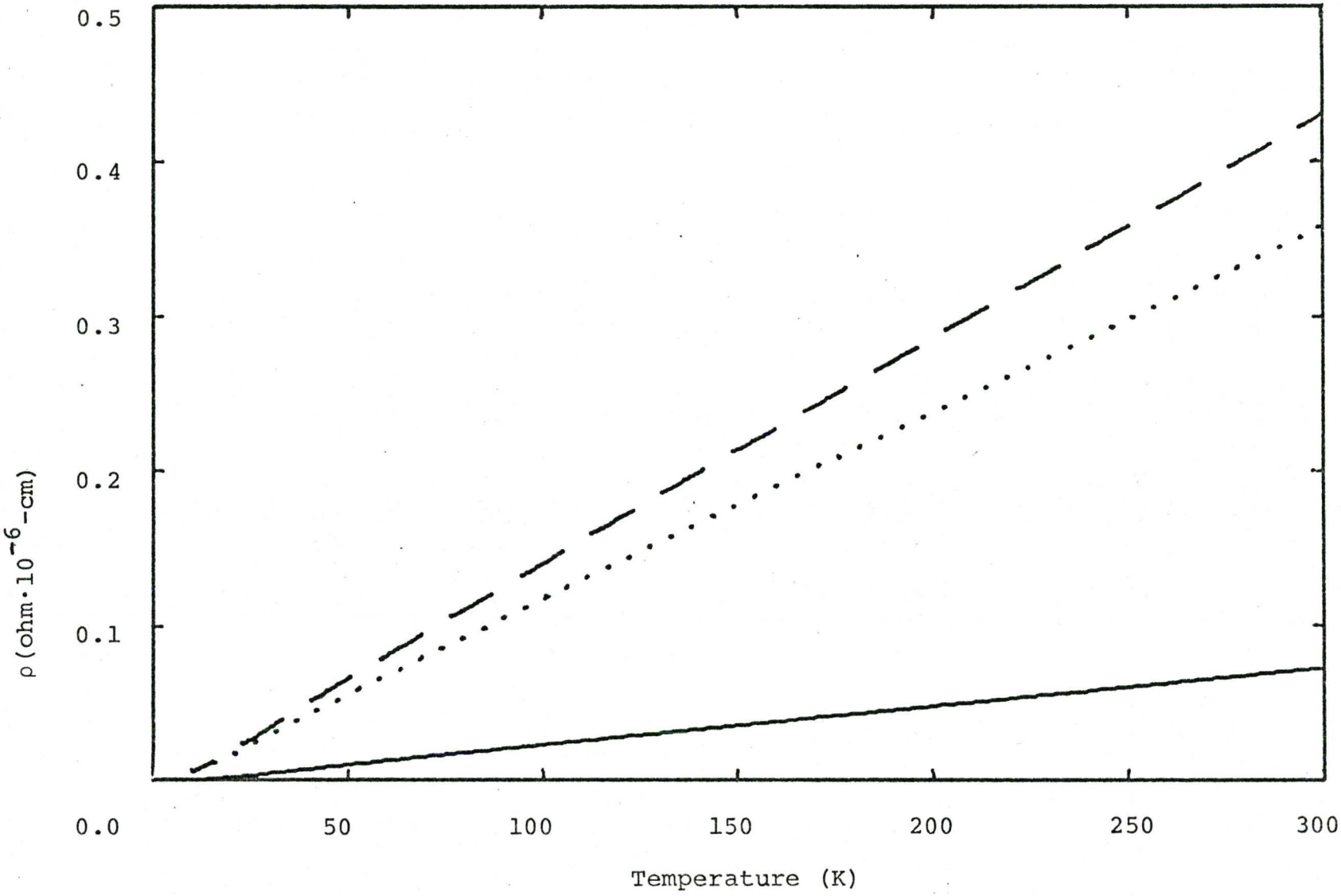
0.5
0.4
0.3
0.2
0.1
0.0
50
100
150
200
250
300
ρ (ohm·10⁻⁶-cm)
Temperature (K)

Fig. 3.8 Residual and impurity contributions to the electrical resistivity of potassium with a sodium impurity

ρ_{pure} ———

$\rho_{pure} + \rho_{residual}$ . . .

$\rho_{pure} + \rho_{residual} + \rho_{impurity}$ - - -

Note: $\rho_{impurity} = \rho_{w\Delta w} + \rho_{\Delta w^2}$

Fig. 3.8

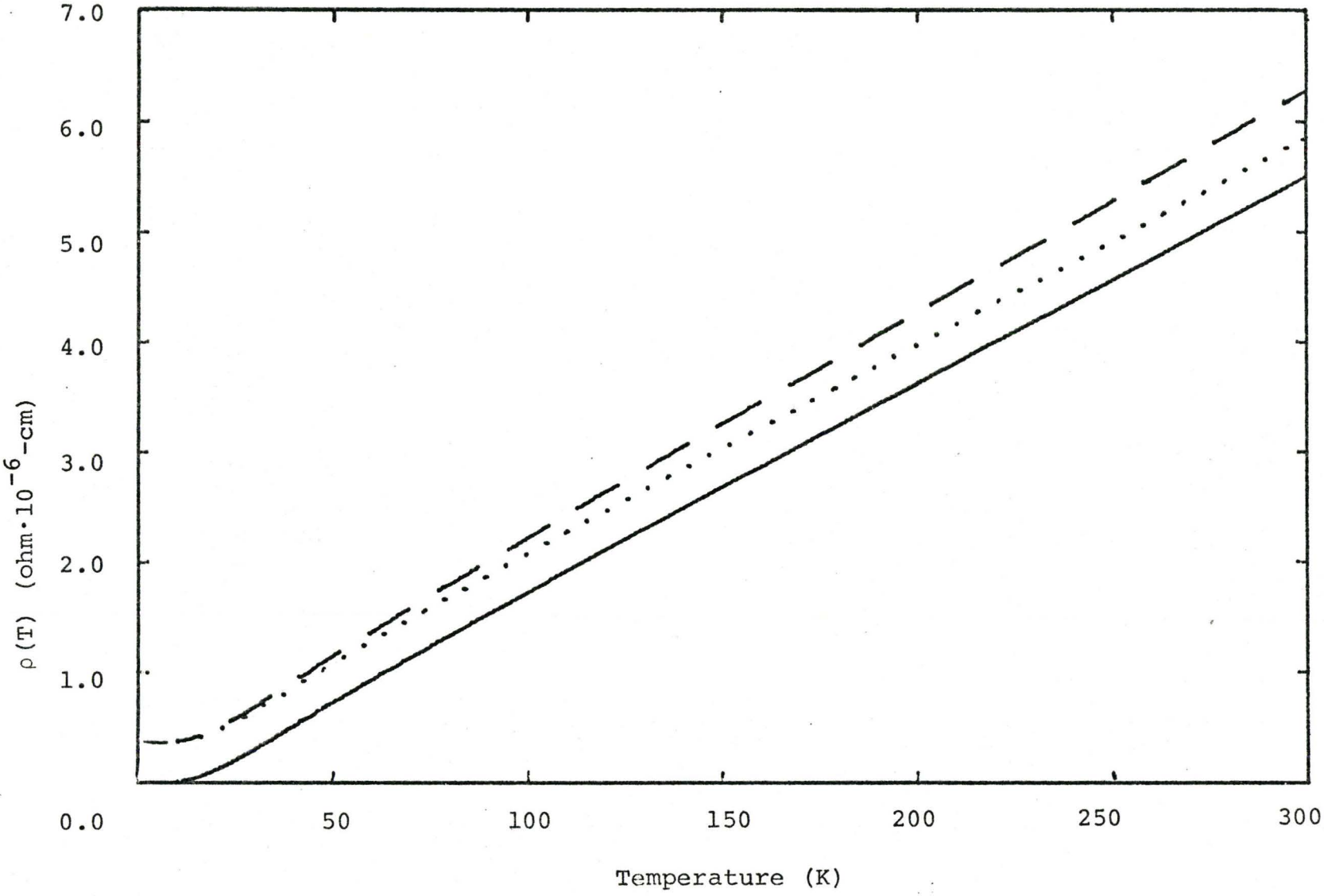
7.0
6.0
5.0
4.0
3.0
2.0
1.0
0.0
50
100
150
200
250
300
ρ(T) (ohm·10⁻⁶-cm)
Temperature (K)

Fig. 3.9 Impurity term contributions to the thermal resistivity for potassium with a sodium impurity

$W_{w\Delta w}$ ———

$W_{\Delta w^2}$ . . .

$W_{w\Delta w} + W_{\Delta w^2}$ - - -

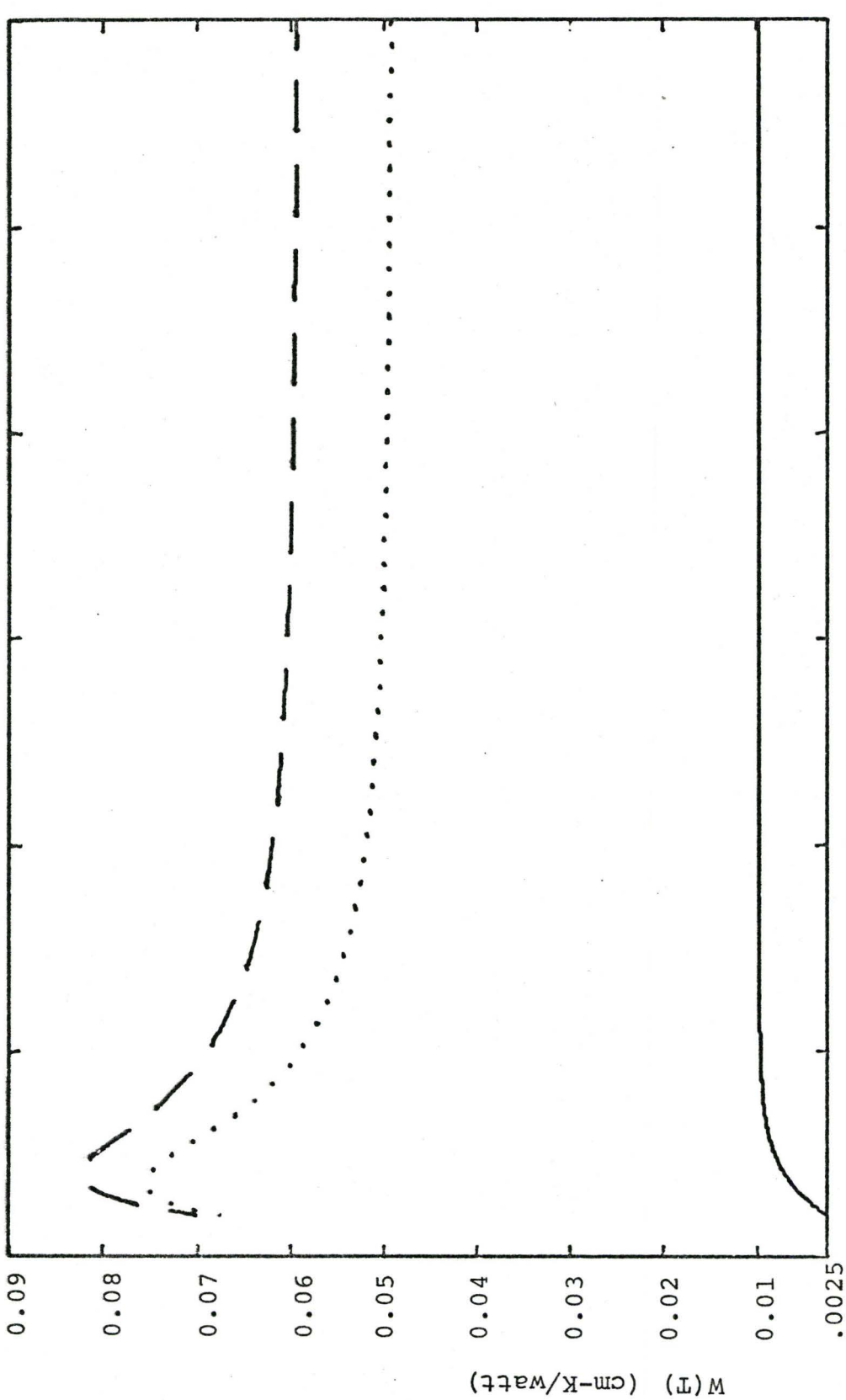
0.09
0.08
0.07
0.06
0.05
0.04
0.03
0.02
0.01
.0025
0
50
100
150
200
250
300
W(T) (cm-K/watt)
Temperature (K)

Fig. 3.9

Fig. 3.10 Impurity contribution to the thermal resistivity for potassium with a sodium impurity

$$\frac{W_{pure}}{W_{pure} + W_{impurity}} \quad \cdots$$

Note: $W_{impurity} = W_{w\Delta w} + W_{\Delta w^2}$

Fig. 3.10

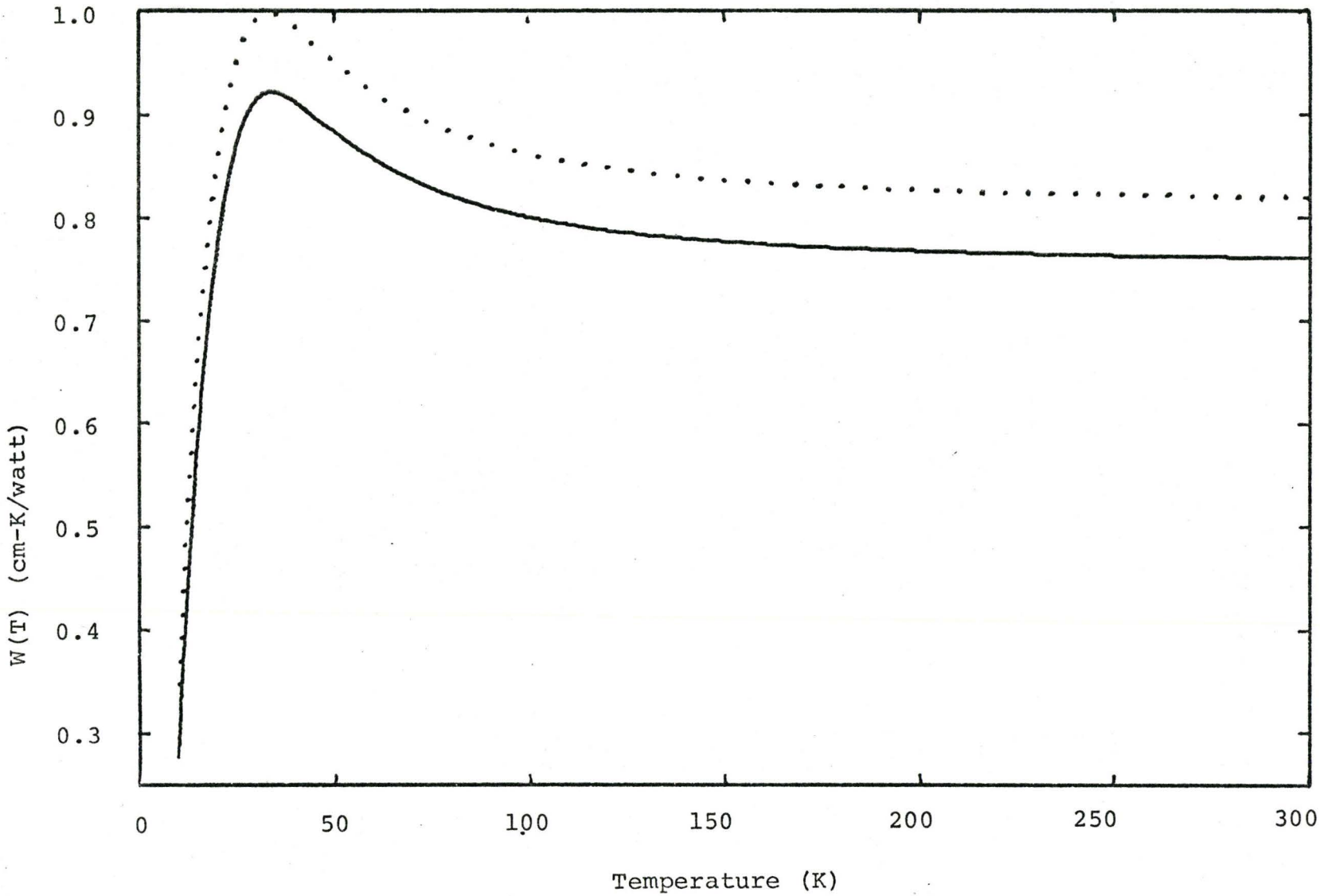
1.0
0.9
0.8
0.7
0.6
0.5
0.4
0.3
W(T) (cm-K/watt)
0
50
100
150
200
250
300
Temperature (K)

Fig. 3.11 Hartree screened Ashcroft pseudopotentials for the system of sodium with a potassium impurity

Sodium ———

R_c = 0.8282 a = 4.2268

Potassium . . .

R_c = 1.0353 a = 4.2268

Fig. 3.11

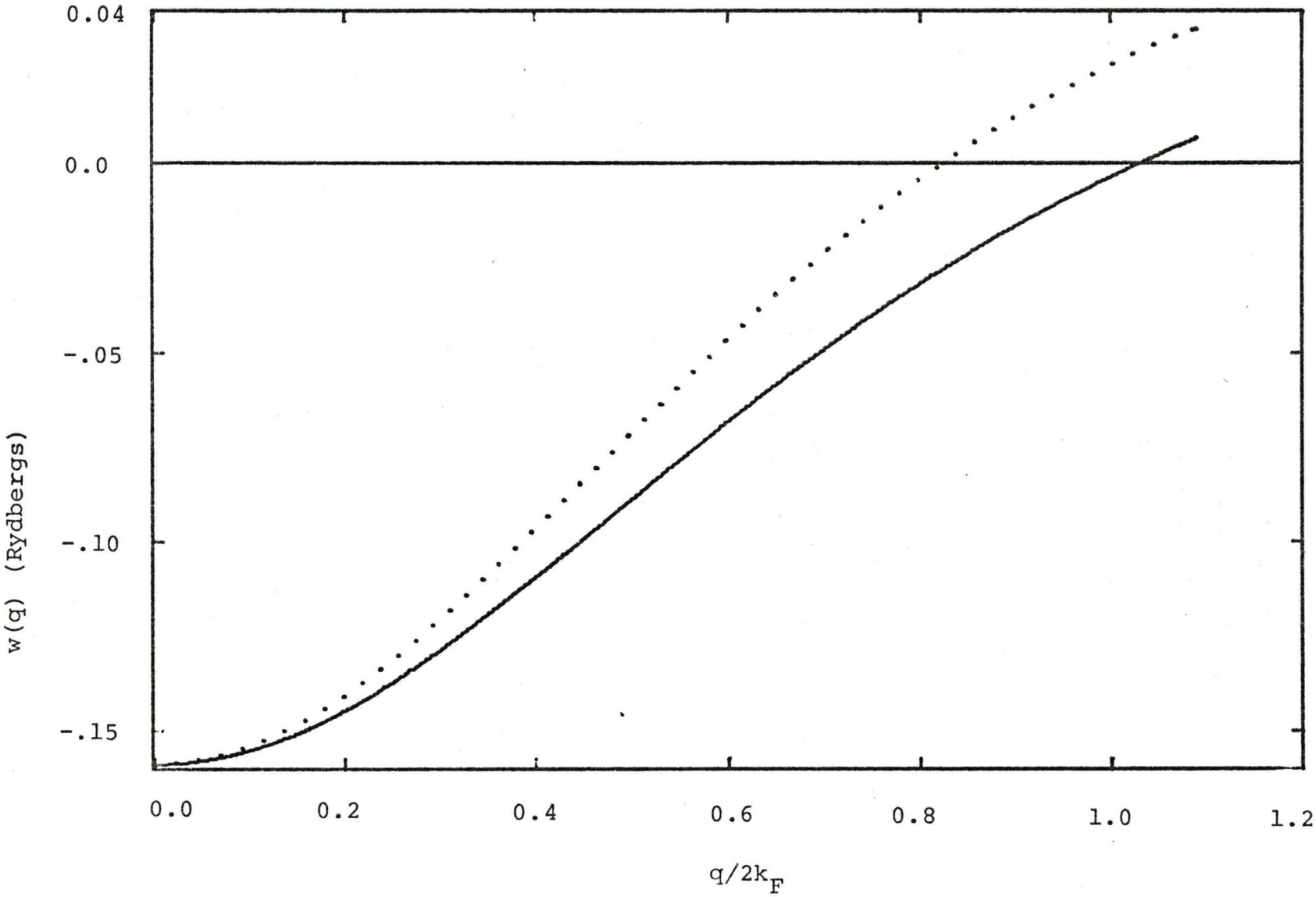

Comparing Figures (3.12) and (3.13) we notice immediately that the auxiliary distributions are negative as a consequence of the negative pseudopotential difference term. This leads, in Figure (3.14), to a negative contribution of the $w(\underset{\sim}{q})\Delta w(\underset{\sim}{q})$ term to the electrical resistivity. Once again, however, the contribution of the $|\Delta w(\underset{\sim}{q})|^2$ term is large. In Figure (3.15) it is clear that the net effect of impurities is that these two terms contribute significantly to the total electrical resistivity. As in the case of the potassium host we have a significant deviation from Matthiessen's Rule which is apparent even at low temperatures.

An analogous situation exists with the thermal resistivity as can be seen in Figures (3.16) and (3.17). Here again the $|\Delta w(\underset{\sim}{q})|^2$ term contribution is of the order of the contribution of the pure thermal resistivity term.

The calculations of this section are an improvement over previous work, notably Kagan and Zhernov (1966) and Bhatia and Gupta (1969) in that detailed numerical evaluation of $w(\underset{\sim}{q})\Delta w(\underset{\sim}{q})$ and $|\Delta w(\underset{\sim}{q})|^2$ terms has been included. In particular, disagreement with Bhatia and Gupta (1969) arises where we find a significant contribution to the electrical resistivity of the $|\Delta w(\underset{\sim}{q})|^2$ term in, for example, the potassium host-sodium impurity system.

Fig. 3.12 Frequency distributions for sodium with a potassium impurity

Hartree screened Ashcroft pseudopotential

$R_c = 0.8282$ $a = 4.2268$

$F(\nu)$ ———

$\alpha^2_{tr}(\nu)F(\nu)$ . . .

$\alpha^2(\nu)F(\nu)$ - - -

Note: $\alpha^2_{tr}(\nu)F(\nu)$ and $\alpha^2(\nu)F(\nu)$ have been scaled up by a factor of 10.

Fig. 3.12

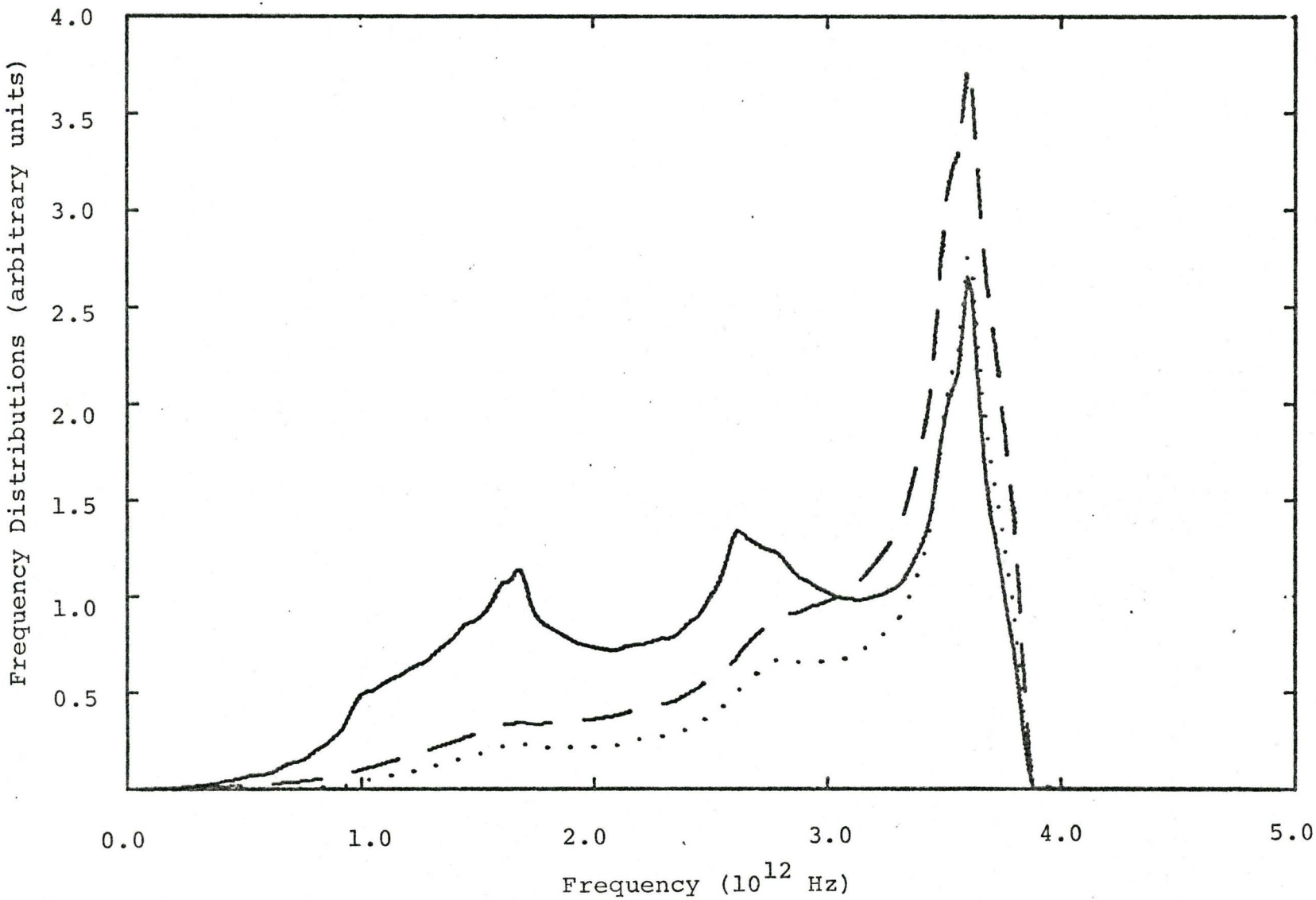
Frequency Distributions (arbitrary units)
4.0
3.5
3.0
2.5
2.0
1.5
1.0
0.5
0.0
1.0
2.0
3.0
4.0
5.0
Frequency (10^{12} Hz)

Fig. 3.13 Auxiliary frequency distributions for sodium with a potassium impurity
Hartree screened Ashcroft pseudopotential

$F(\nu)$ ———

$\alpha'^2_{tr}(\nu)F(\nu)$ . . .

$\alpha'^2(\nu)F(\nu)$ - - -

Note: $\alpha'^2_{tr}(\nu)F(\nu)$ and $\alpha'^2(\nu)F(\nu)$ have been scaled up by a factor of 10.

Fig. 3.13

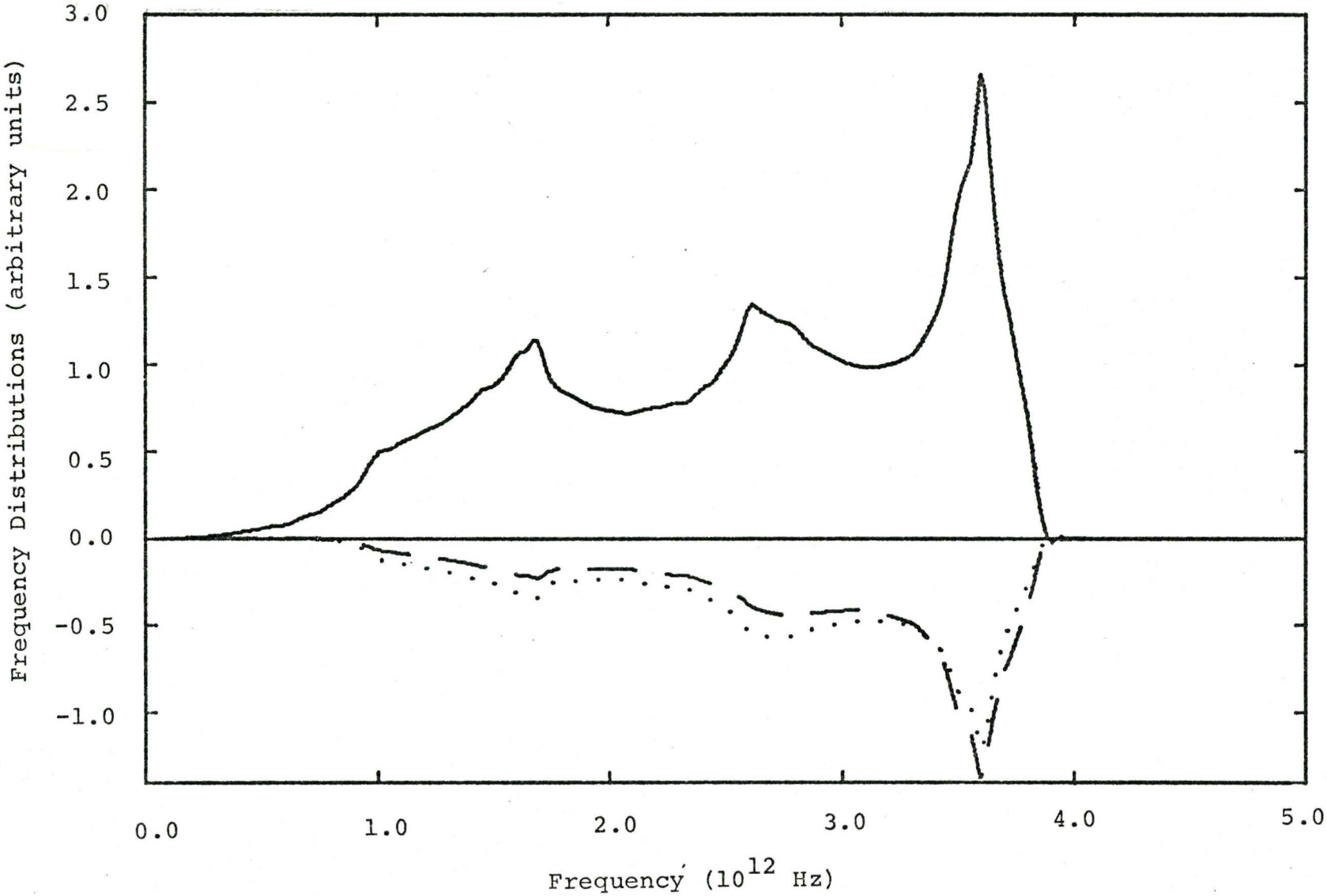
3.0
2.5
2.0
1.5
1.0
0.5
0.0
-0.5
-1.0
Frequency Distributions (arbitrary units)
0.0
1.0
2.0
3.0
4.0
5.0
Frequency (10^{12} Hz)

Fig. 3.14 Impurity term contributions to the electrical resistivity for sodium with a potassium impurity

$\rho_{w\Delta w}$ ———

$\rho_{\Delta w^2}$ . . .

$\rho_{w\Delta w} + \rho_{\Delta w^2}$ - - -

Fig. 3.14

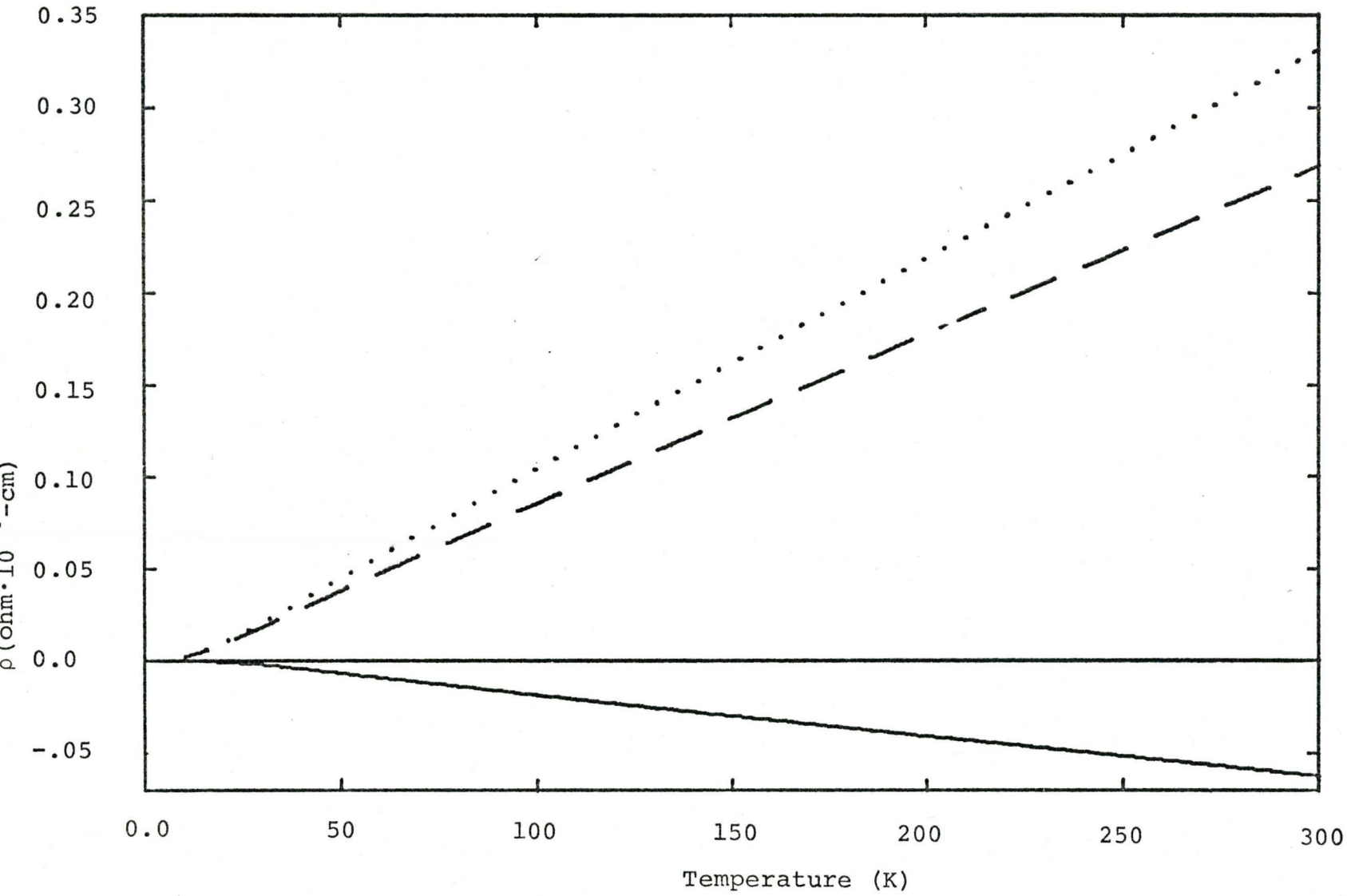
0.35
0.30
0.25
0.20
0.15
0.10
0.05
0.0
-.05
ρ(ohm·10 -cm)
0.0
50
100
150
200
250
300
Temperature (K)

Fig. 3.15 Residual and impurity contributions to the electrical resistivity of sodium with a potassium impurity

ρ_{pure} ———

$\rho_{pure} + \rho_{residual}$ . . .

$\rho_{pure} + \rho_{residual} + \rho_{impurity}$ - - -

Note: $\rho_{impurity} = \rho_{w\Delta w} + \rho_{\Delta w^2}$

Fig. 3.15

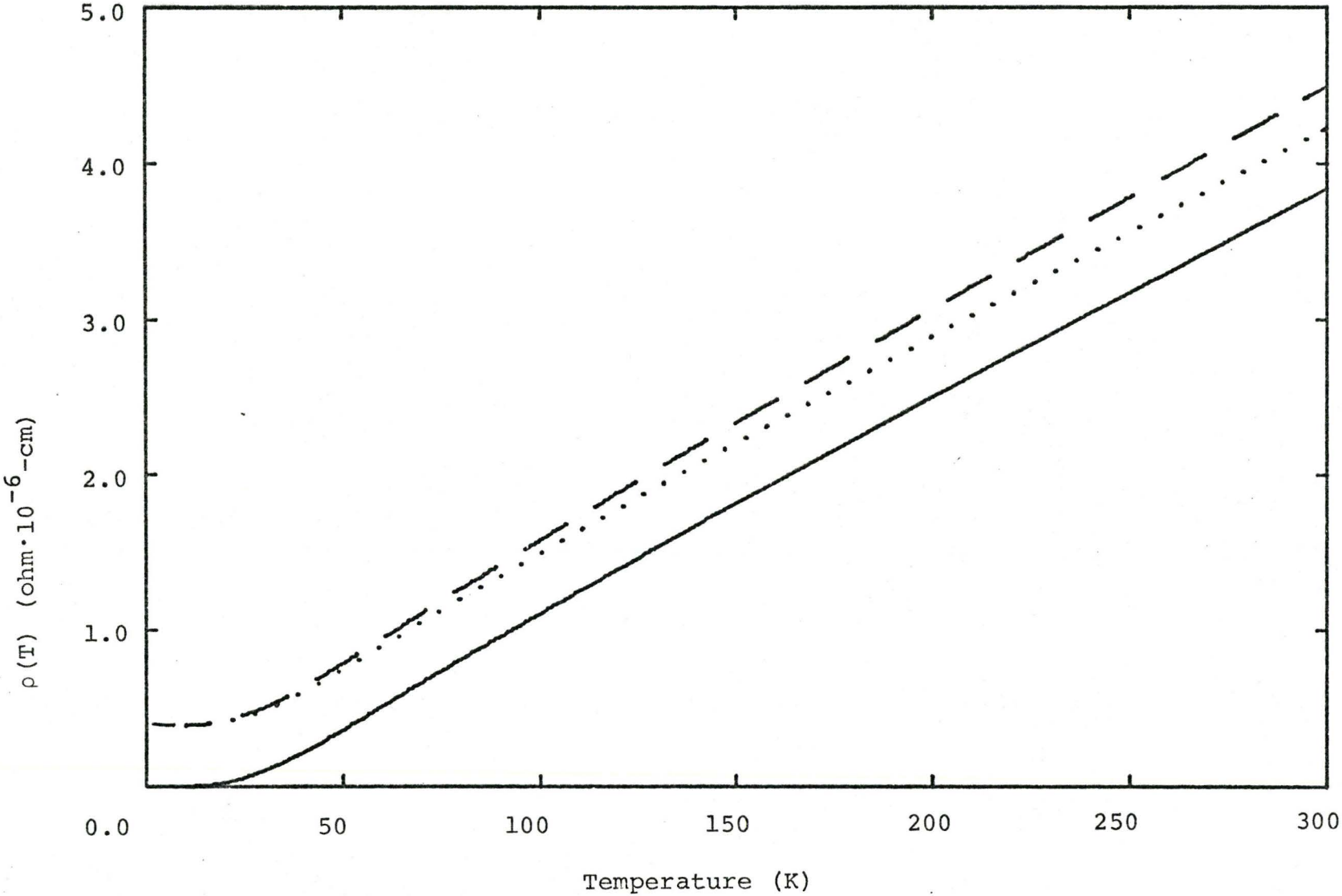
5.0
4.0
3.0
2.0
1.0
0.0
50
100
150
200
250
300
ρ(T) (ohm·10⁻⁶-cm)
Temperature (K)

Fig. 3.16 Impurity term contributions to the thermal resistivity for sodium with a potassium impurity

$W_{w\Delta w}$ ———

$W_{\Delta w^2}$ . . .

$W_{w\Delta w} + W_{\Delta w^2}$ - - -

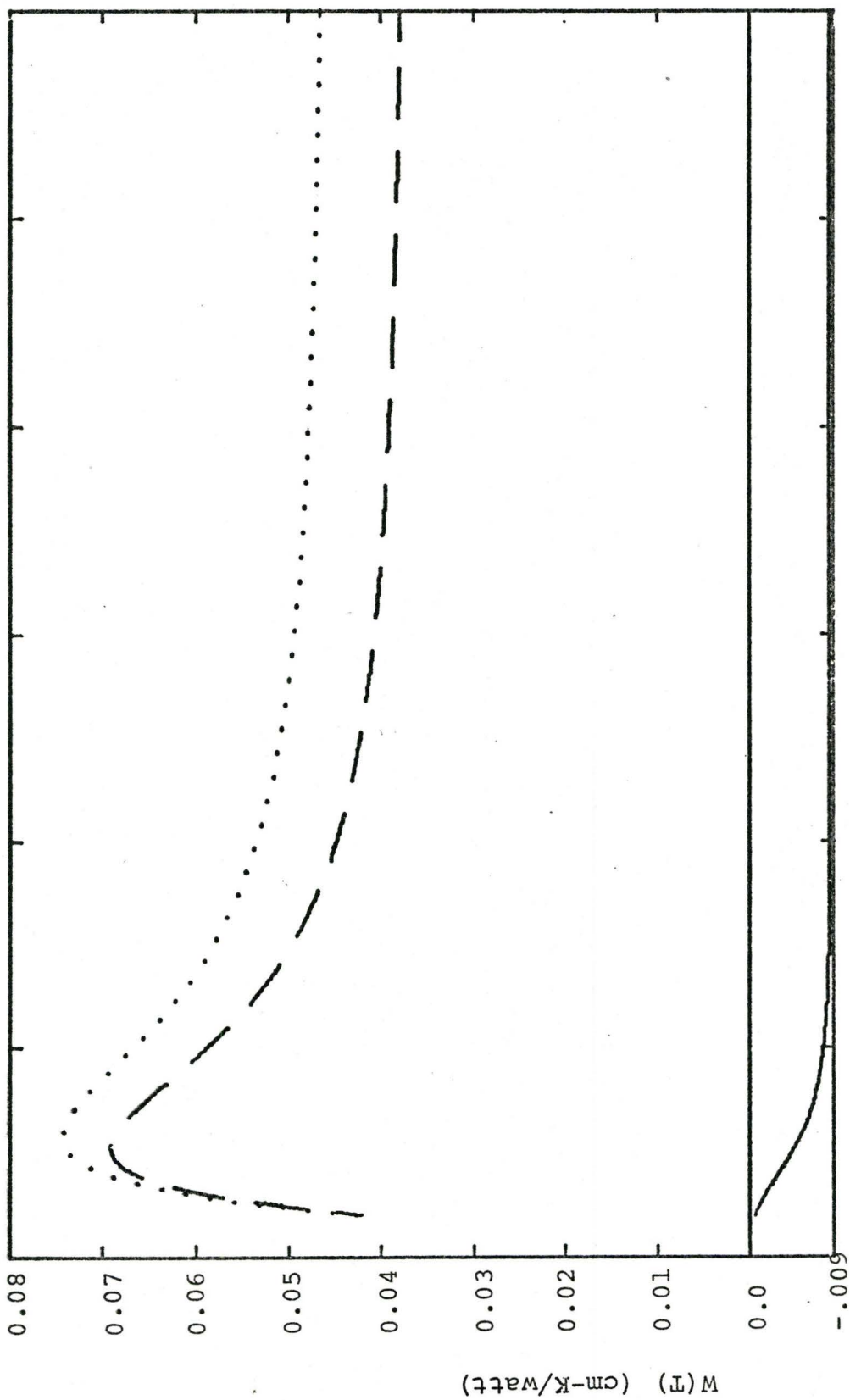
0.08
0.07
0.06
0.05
0.04
0.03
0.02
0.01
0.0
-.009
W(T) (cm-K/watt)
0.0
50
100
150
200
250
300
Temperature (K)

Fig. 3.16

Fig. 3.17 Impurity contribution to the thermal resistivity for sodium with a potassium impurity

W_{pure}

$W_{pure} + W_{impurity}$

Note: $W_{impurity} = W_{w\Delta w} + W_{\Delta w^2}$

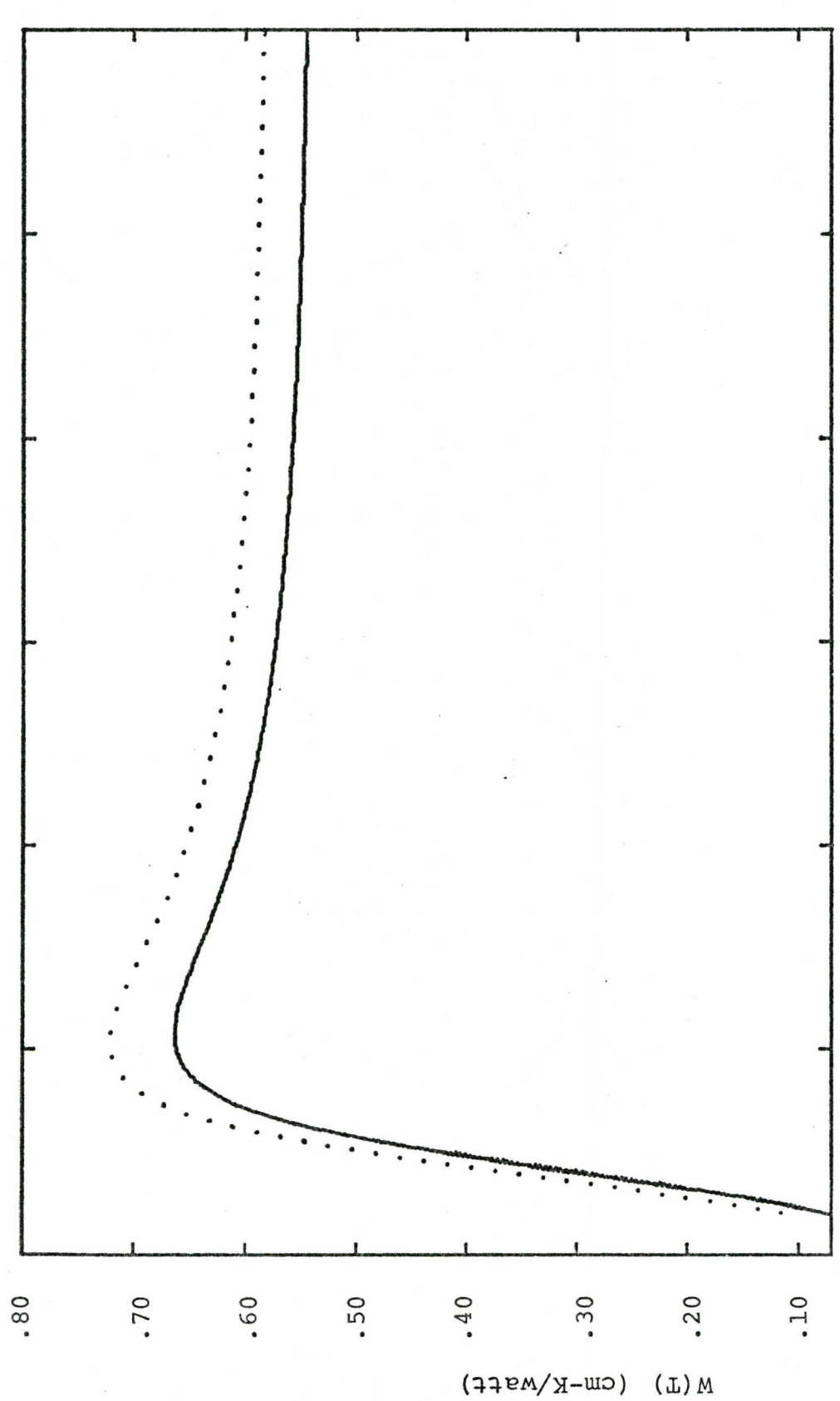
.80
.70
.60
.50
.40
.30
.20
.10
W(T) (cm-K/watt)
0.0
50
100
150
200
250
300
Temperature (K)

Fig. 3.17

In conclusion it should be emphasized that the calculation shows unambigously that the change in the electron phonon interaction due to the addition of impurities leads to significant and measurable deviations from Matthiessen's Rule at the 1% concentration level and these deviations should be measurable. It is hoped that the results will stimulate further experiment.

APPENDIX A

COMPUTER PROGRAMME FOR COMPUTING PHONON FREQUENCY DISTRIBUTIONS

A.1 General

The computer programme described in this appendix calculates weighted isotropic effective phonon frequency distributions. It is based on programme GNU which was originally written by L. J. Raubenheimer and G. Gilat to calculate the phonon density of states for cubic crystals. The material in this appendix applies specifically to a BCC version held by the Theoretical Physics Group at McMaster University. Several other similar versions exist for different crystal structures including:

body centred cubic	BCC
face centred cubic	FCC
simple cubic hexagonal close packed	HCP .

These versions all assume only one atom per unit cell, and that the Born-von Kármán force constant model is used. As has been pointed out by Gilat and Raubenheimer (1966), the programme can be readily generalized for more complicated systems.

In its present form the programme reflects the philosophy that separate parts of the calculation should

exist as separate subroutines, called in the appropriate sequence by the main programme. This allows the logical subdividions of the calculation to become apparent and facilitates understanding of the operation of the programme. It also adds flexibility to the programme in that modifications may be made to particular parts of the calculation simply by removing and adding subroutines.

The programme is written in Fortran IV and is operational on the McMaster CDC 6400. Although some non-standard CDC Fortran is used, the code could be made to run on other machines with only minor modifications.

A.2 Programme Description

Main Programme PHNFRQD

The main programme serves the principle function of controlling the sequence of the calculation by calling subroutines in the order required. Other functions are listed as follows:

1. Definition and calculation of constants used in the subroutines.
2. Input of data and output of intermediate results such as frequency distributions and pseudopotentials.

Function ASPVDF

This function calculates screened Ashcroft pseudopotentials and allows for a variable dielectric function. The type of screening is controlled by the parameters which appear on the pseudopotential data card read by the main programme. The function returns the pseudopotential in Rydbergs and will accept values of $\tilde{q}$, momentum transfer, between 0 and $2k_F$. Of the dielectric functions considered, the Lindhart (simple screening) and the Singwi (addition of terms for many body effects), appear to be the most interesting.

Subroutine CALCUL

This subroutine performs the bulk of the calculation. Its principle functions are listed as follows:

1. CALCUL subdivides reciprocal space into a mesh of small cubes. The dynamical matrix is then diagonalized everywhere in each cube by a linear extrapolation technique. (This diagonalization is carried out by Subroutine FREQ and the subroutines it calls.) In calculating $F(\nu)$, diagonalization is necessary only within the FBZ. In order to include umklapp processes when calculating distribution functions this process must be carried out to a radius of $2k_F$. This is accomplished using a series of geometrical transformations which are different for each crystal structure and which are contained in Subroutine CALCUL. It should be noted that running indices IMIN and IMAX are used so that a finer mesh spacing can be achieved closer to the origin where the extrapolation technique is less accurate.
2. Different weights are assigned to cubes in the mesh depending on whether or not they lie entirely or only partly with the FBZ extended to $2k_F$. This is necessary for the linear extrapolation technique.

3. Pseudopotential factors and other frequency distribution weighting factors are calculated. The frequency distributions are multiplied by weighting factors after the frequency histograms are constructed by Subroutine SWEEP.

Subroutine ORGDTA

This subroutine acts on the distribution functions by doing the following:

1. When the distributions are constructed the first 50 channels are for negative frequencies. These first 50 channels of the frequency distribution which will become $\alpha^2(\nu)F(\nu)$, are then printed out by Subroutine ORGDTA as a check on the validity of the calculation. They should obviously all be zero or nearly zero. The subroutine then shifts all of the distributions so that the first positive frequency is channel one.
2. Subroutine ORGDTA then calculates the normalization factor and normalizes all of the distributions. The normalization factor is calculated using equation (A.1),

$$\int F(\nu)d\nu = 3 \quad , \tag{A.1}$$

where the integration is performed over all channels of the distribution. The total number of channels in the distributions in a given calculation is determined by the factor SM/DVA + 1.

3. Depending on the value of parameter NRNORM, Subroutine ORGDTA will renormalize the first NRNORM channels of the distribution.

Subroutine ALPHA

Using the distribution functions calculated elsewhere in the programme this subroutine calculates and prints out the following results:

1. $\alpha^2(\nu)F(\nu)/F(\nu)$

2. $\alpha^2(\nu)F(\nu)/\nu$

3. $\int (\alpha^2(\nu)F(\nu)/\nu)d\nu$,

where the integral is performed over the total number of channels in the distribution.

Subroutine WRT

This subroutine serves the sole purpose of tabulating frequency distributions, and other functions in a convenient format for output on the line printer.

Subroutine CONST

The main purpose of this subroutine is to prevent unnecessary repetition of calculations in Subroutine ELEM. In particular, the force constants PX(I) often appear with the same numerical factors in the elements of the dynamical matrix. These numerical factors are incorporated into the force constants in CONST. The subroutine also calculates some additional constants which are used elsewhere in the programme.

Subroutine FREQ

This subroutine, together with Subroutines ELEM, DIAG3 and GRAD performs the procedure described by equations (1.27) to (1.32) in Section 1.2 on numerical techniques. For a given $\underset{\sim}{q}$ [Q] FREQ calls ELEM to establish the dynamical matrix $D^0_{\alpha\beta}(\underset{\sim}{q})$ [A], where the parameter used in the programme is included in square brackets for clarity. Subroutine DIAG3 diagonalizes $D^0_{\alpha\beta}(\underset{\sim}{q})$ and stores the eigenvalues in [V] and the eigenvectors in [EV]. FREQ then

calls ELEM to obtain the modified dynamical matrix $D^{\gamma}_{\alpha\beta}(\underset{\sim}{q} + \hat{e}_{\gamma}\delta q_{\gamma})$ [AA] and then the change in the dynamical matrix $\Delta^{\gamma}_{\alpha\beta}(\underset{\sim}{q})$ which is stored as array [DA]. Subroutine GRAD is then called to calculate successively each of the three cartesian components of the gradient of frequency [GD1, GD2, GD3] using the method shown by equations (1.30) to (1.32). The frequencies [V] which these gradients are used to calculate, are used in SWEEP (called from CALCUL) to construct the frequency histograms. They are also employed as weighting functions for some of the distributions in CALCUL.

Subroutine ELEM

This subroutine calculates the elements of the dynamical matrix $D^{0}_{\alpha\beta}(\underset{\sim}{q})$ [A]. If other than the Born-von Kármán theory were used, this subroutine and part of CONST would have to be changed.

Subroutine DIAG3

This subroutine finds the eigenvalues and eigenvectors of a real symmetric 3×3 matrix.

Subroutine GRAD

This subroutine calculates one cartesian component of the gradient of each of the eigenfrequencies. The method is that of equations (1.30) to (1.32) of Section 1.2. The eigenvector matrix $U(\underset{\sim}{q})$ and the change in the dynamical matrix $\Delta^{\gamma}_{\alpha\beta}(\underset{\sim}{q})$ are given in the subroutine by EV and A respectively.

Subroutine SWEEP

Subroutine SWEEP uses the eigenfrequencies and gradients obtained at the centre of each small cube and performs a linear extrapolation throughout the cube. The method is illustrated by equation (1.33). SWEEP then sorts the frequencies into a histogram which, when multiplied by appropriate weighting factors in CALCUL and ORGDTA, becomes a frequency distribution function.

It should be noted at this point that new frequency distribution functions can readily be added to the programme. The additions would be required in SWEEP, CALCUL and ORGDTA and are obvious from the context of these subroutines.

Resistivity Subroutines

In this section we want to consider subroutines, such as those for calculating electrical and thermal resistivity, which use the frequency distribution functions calculated elsewhere in the programme.

Often the property calculated is temperature dependent and this is usually included by placing most of the subroutine within a loop and incrementing the temperature. Factors used in these subroutines are best calculated as separate functions such as function RESRES for the residual resistivity. The gaussian integration Subroutine QG32D1 is employed when functions are integrated. It should be emphasized that including separate calculations as separate subroutines in the way described above allows for the greatest flexibility when it becomes necessary to modify or change the calculations.

Plotting Subroutines

Subroutines PLOTLP and PLOTOP allow for the plotting of distributions, pseudopotentials and other functions on the line printer and offline plotter respectively. By defining appropriate arrays and parameters in the programme, graphical output can be produced by simply inserting a call statement for the relevant plotting subroutine.

A.3 Input Parameters

The following is a detailed description of the input parameters, all of which are read in by the main programme PHNFRQD. If graph plotting Subroutines PLOTOP and PLOTLP are used with the programme, then title cards are read when these subroutines are entered.

1st Data Card

Title for the output (16A5 format)

2nd Data Card

NSFB (crystal structure parameter)

= 1 simple cubic

= 2 face centred cubic

= 3 body centred cubic

Note: This parameter controls the establishment of running conditions over the appropriate 1/48 irreducible sector of the FBZ, (hereafter called the irreducible zone or IZ), which are different for the different crystal structures. NSFB has the above effect in Subroutine CALCUL and also causes special action in Subroutines CONST and ELEM.

NNN = dimension of dynamical matrix
= 3 × (number of atoms per unit cell).

NFC = number of force constants to be read on the fourth data card(s).

KK = a number which determines the "fineness" of the mesh dividing the IZ. The mesh number or number of slices into which q_x is initially divided is JIMAX in the programme and is weighted as follows:

JIMAX = KK simple cubic
4KK FCC
2KK BCC

KK has a significant influence on the resolution of the distribution and hence on the computation time.

KG This parameter controls special print output from the programme.

KG = positive - no special output
= negative or zero - special output as follows from Subroutine CALCUL (once for each time through the subroutine loop)

NS = mesh point sequence number

I = loop index on IMIN, IMAX (IZ) loop

K = loop index on I, J (IZ) loop

U(1), U(2), U(3) = weighting factor for 3 components of $F(\omega)$

QA, QB, QC = original $\underset{\sim}{q}$ components in FBZ (before transformations)

V(1), V(2), V(3) = three components of the frequency $\omega(\underset{\sim}{q};\lambda)$

from Subroutine SWEEP (once for each time through the subroutine loop on I, I = 1, 3)

V(I) = i^{th} components of the frequency $\omega(\underset{\sim}{q};\lambda)$

GRD = absolute value of gradient frequencies

AL(1), AL(2), AL(3) = direction cosines of gradient vector

DELW = thickness of slice into which cubes are divided

W1 (|W1| is the distance from cube centre to the first corner)

if W1 > 0 : 6 sided case

W1 < 0 : 4 sided case

VOLUME = correct volume of the cube

DIFF = error made in finding the volume by adding all volume elements together

NDEL = the number of frequency channels to which this extrapolation contributes.

IMIN = iteration lower bound usually set to zero and calculated by programme - controls looping in Subroutine CALCUL.

IMAX = iteration upper bound usually set to zero and calculated by programme - controls looping in Subroutine CALCUL.

NRNORM = parameter controlling distribution renormalization in Subroutine ORGDTA.

NRNORM = 0 no renormalization

NRNORM > 0 the first NRNORM channels of distribution will be renormalized

Note: The renormalization is only employed in the FCC version of the programme and in this version applies only to $\alpha^2(\nu)F(\nu)$ and $\alpha^2_{tr}(\nu)F(\nu)$.

DVA = channel width of histogram in units of 10^{12} Hz.

XM = maximum frequency of histogram in units of 10^{12}Hz.

DQ = Δq for computing $\nabla\nu$ - usually taken to be 0.0001.

Note: The numerical process employed here is described in Chapter I, see equation (1.33).

3rd Data Card

AMAS(1) = atomic mass in AMU, and later redefined as variable ATMA.

Note: The other three variables, AMAS(I), are retained from an earlier version of the programme and are not used. They are entered on the data card as zeros.

4th Data Card

PX(I), I = 1, NFC These data cards contain the force constants, four to a card. The number of entries is

controlled by NFC which was read in on the 2nd Data Card.

5th Data Card

ALATC = lattice constant in angstroms.

ZCH = charge number.

6th Data Card

Pseudopotential parameters are read in on this card(s). Statements suitable for reading in Shaw or Heine-Abarenkov pseudopotential parameters may be included using the variables PSEUD(I) or PSEUD2(I). In Subroutine CALCUL pseudopotential weighting factors may be calculated using these variables. The Ashcroft pseudopotential may also be constructed using the following variables which are read in on this card(s).

ISP = this parameter determines the type of screening used with the Ashcroft pseudopotential.

RCORE = core radius of the Ashcroft pseudopotential.

RS = density of states parameter characteristic of Singwi parameters A and B. In this version of Function ASPVDF it is not used in the calculation.

(RS = 0 when ISP $\neq$ 5).

A, B Singwi parameters used when Singwi screening is applied to the Ashcroft pseudopotential (ISP = 5).

(A = B = 0 when ISP $\neq$ 5).

RCIMP = core radius of impurity atom Ashcroft pseudopotential.

Note: 1. If other than the Ashcroft pseudopotential is employed, the pseudopotential is calculated in Subroutine CALCUL. If the Ashcroft pseudopotential is used, it is calculated with appropriate screening by Function ASPVDF.

2. If host-impurity calculations are performed by the programme, then RCIMP applies to the impurity and all other parameters apply to the host, including RCORE.

7th Data Card

Additional cards may be read in containing titles for plotted output. Subroutines PLOTLP and PLOTOP have been used to plot distribution functions and pseudopotentials on the line printer and offline plotter respectively.

REFERENCES

N. W. Ashcroft and D. C. Langreth, Phys. Rev. 159 (1967) 500.

G. Baym, Phys. Rev. 135 (1964) 1691.

A. B. Bhatia and O. P. Gupta, Phys. Lett. 29A (1969) 358.

J. P. Carbotte and R. C. Dynes, Phys. Rev. 172 (1968) 476.

J. G. Cook, M. P. Van Der Meer and M. J. Laubitz, Can. J. Phys. 50 (1972) 1386.

R. C. Dynes, Ph.D. Thesis, McMaster University, Hamilton, Ontario, Canada (1968) unpublished.

R. C. Dynes and J. P. Carbotte, Phys. Rev. 175 (1968) 913.

J. W. Ekin and A. Bringer, Phys. Rev. B 7 (1973) 4468.

G. Gilat and G. Dolling, Phys. Lett. 8 (1964) 304.

G. Gilat and L. J. Raubenheimer, Phys. Rev. 144 (1966) 390.

B. Hayman and J. P. Carbotte, Can. J. Phys. 49 (1971) 1952.

Y. Kagan and A. P. Zhernov, Zh. Eksperim. i Teor. Fiz. 50 (1966) 1107; Soviet Phys. JETP 23 (1966) 737.

F. Kus and J. P. Carbotte, J. Phys. F. 3 (1973) 1828.

D. L. Price, W. Shyu, K. S. Singwi and M. P. Tosi, Argonne National Lab. Report, ANL-7761 (1970).

K. S. Singwi, A. Sjolander, M. P. Tosi and R. H. Land, Phys. Rev. B 1 (1970) 1044.

P. N. Trofimenkoff, Ph.D. Thesis, McMaster University, Hamilton, Ontario, Canada (1969) unpublished.

P. T. Truant, Ph.D. Thesis, McMaster University, Hamilton, Ontario, Canada (1972) unpublished.